SLAC – PUB – 4379
August 1987
(A/E/T)

AN INTRODUCTION TO BEAMSTRAHLUNG AND DISRUPTION*

PISIN CHEN

Stanford Linear Accelerator Center
Stanford University, Stanford, California 94305

TABLE OF CONTENTS

Lecture given at US–CERN Joint Topical Course
on "Frontiers of Particle Beams,"
South Padre Island, Texas, Oct. 23–29, 1986

* Work supported by the Department of Energy, contract DE – AC03 – 76SF00515.

AN INTRODUCTION TO BEAMSTRAHLUNG AND DISRUPTION

PISIN CHEN

Stanford Linear Accelerator Center
Stanford University, Stanford, California 94305

1. INTRODUCTION

To achieve enough luminosity for high energy physics experiments, it is inevitable to focus the colliding e^+e^- beams down to miniscule dimensions at the interaction point in linear colliders. In the world's first of such accelerators, the Stanford Linear Collider (SLC), beam size at the interaction point is designed to be $\sigma_x = \sigma_y = 1.65\ \mu$m, and $\sigma_z = 1$ mm [1]. For the next generation of linear colliders at the range of 1 TeV in center-of-mass energy the beam size would be even smaller. The high density of charged relativistic particles would provide strong electromagnetic fields viewed by the particles of the oncoming beam, while the particles in the same bunch have no effect among each other because of the cancellation of Lorentz forces between the electric and the magnetic components to the accuracy of the order of $1/\gamma$. The bending of particle trajectories under the influence of these EM fields provided by the oncoming beam is called disruption. During bending particles would radiate, causing an energy loss of the beam; this is called beamstrahlung. Both effects are important to the design of linear colliders [2, 3].

In this lecture we review the current understanding of the beam-beam interaction in e^+e^- linear colliders. Strictly speaking, the two effects, disruption and beamstrahlung, during beam-beam interaction are coupled. This is self-evident because without deflection there would be no radiation, and with radiation during bending the remaining trajectory of particles would not be the same. Fortunately, in a large range of beam parameters the average disruption angles are rather small, and the emission of hard photons are relatively rare. For these reasons the two effects can be isolated from each other to the first degree of accuracy, and our study of the issue can be greatly simplified. This happens also to be the development historically. In sec. 2 we discuss the effects associated with disruption with negligible beamstrahlung. Here, an important parameter, the disruption parameter D, is introduced. We then discuss the maximum and *rms* disruption angles. The analytic scaling laws for $D \gg 1$ and $D \ll 1$ are then compared with simulation results. Next we investigate the enhancement of luminosity due to disruption. Together with the aspect ratio $R \equiv \sigma_x/\sigma_y$, the two parameters define a scaling law for luminosity enhancement, H_{D1}, due to the mutual pinching of the e^+e^- bunches where the effective beam size $\sigma_x\sigma_y$ is reduced. In addition to the luminosity enhancement arised from the overall reduction of the beam size, there is a second source for the enhancement that comes from the extremely high particle density at the focal point inside the oncoming bunch. This second enhancement, H_{D2}, becomes dominant over H_{D1} when $D \gtrsim 1$, and is a function of the initial emittance which is characterized by the parameter $A \equiv \sigma_x/\beta^*$, where β^* is the β-function at the interaction point.

Next we discuss beamstrahlung with negligible disruption in sec. 3. First we review the nature of beamstrahlung by describing the novel features of the problem. These specific features are then compared with the known radiation phenomena with emphasis on their similarities and differences. We argue that, in certain parameter range, the radiation mechanism of beamstrahlung is synchrotron radiation in nature. By this we mean the emission of a photon is induced by the interaction between the radiating particle and a collection of target particles via its macroscopic EM field. Again, an important parameter, the beamstrahlung parameter Υ, is introduced. For the case $\Upsilon \ll 1$, typical energy of the photons is much smaller than the initial energy of the radiating particle and this is called the classical regime. On the contrary, when $\Upsilon \gg 1$, photons tend to carry away a substantial fraction of the radiating particle energy; this is the quantum regime. For intermediate values of Υ, i.e., $0.1 \lesssim \Upsilon \lesssim 100$, the radiation is in the transition regime. We first derive the synchrotron radiation intensities from a semi-uniform field in the classical and quantum regimes. These expressions reproduce all the well-known formulas for a uniform field. We then review the concept of radiation formation length ℓ_R and argue that the effect of granularity of the target bunch is not observable in the quantum regime. Next we focus on the fact that in the problem of beamstrahlung the target field is longitudinally inhomogeneous. To be correct it is necessary to include the effect due to the variation of the field when $F \equiv \ell_R/\sigma_z \lesssim 1$. In the extreme limit where $F \gg 1$, the radiation mechanism would depart from the characteristics of synchrotron radiation and transform into that of bremsstrahlung.

The average fractional energy loss $\langle\epsilon\rangle$ in beamstrahlung is then calculated explicitly. In the semi-uniform field approximation, one novel aspect is that in the nonclassical regime $\langle\epsilon\rangle$ is "reduced" from what the classical radiation formula would predict based on the same value of Υ. The first beamstrahlung reduction factor $H_{\Upsilon 1}$ is introduced to describe this relative change. When the slope effect is included, we see a second beamstrahlung reduction effect, described by $H_{\Upsilon 2}$. The quantum fluctuation due to finite number of radiated photons in various beamstrahlung quantities are listed as an appendix.

The emphasis of this article is on the fundamental physics of the phenomena during beam-beam interaction. We therefore limit the scope to single e^+e^- bunch pairs with head-on collision. Many important issues, such as kink instability during multi-bunch crossings [4] and collision at an angle [5], are not discussed. Even within the scope of single bunch pair head-on collision, we have to regrettably limit ourselves to the approximation of decoupling disruption and beamstrahlung. The real issues of beam-beam interaction concerning beamstrahlung with disruption, and disruption with beamstrahlung, are not covered in this lecture. The former issue has to do with finding a more realistic effective Υ that includes the pinching of the beam area, while the latter issue relates to the maximum disruption angles from particles that suffer severe radiation losses. With this grand picture in mind, our discussion in this paper should be regarded only as an introduction to the subject of linear collider beam-beam interaction which is very rich in new physics. Throughout this paper we adopt the convention $c = \hbar = 1$.

2. DISRUPTION WITH NEGLIGIBLE BEAMSTRAHLUNG

Let us recall that the nominal luminosity for head-on collision of two gaussian bunches is

$$\mathcal{L}_0 = \frac{N^2 f_r}{4\pi\sigma_x\sigma_y} \quad , \tag{2.1}$$

where N is the number of particles per bunch and f_r is the bunch collision rate. When including the disruption effect, the effective beam area is smaller, which in turn enhances the luminosity. This can be parameterized by a pinch enhancement factor H_D

$$\mathcal{L} = H_D\,\mathcal{L}_0 \quad . \tag{2.2}$$

In this section we review the effects of disruption during beam-beam interaction with negligible beamstrahlung energy loss.

2.1 Focusing Effect and the Disruption Parameter

When an electron bunch collides with a positron bunch, the collective fields from the particles in one oncoming bunch act like a lens to focus the particles in the other bunch toward the axis. The space charge force from the like particles in the same bunch is negligible to the accuracy of the order of $1/\gamma$, where γ is the Lorentz factor of the relativistic bunch in the e^+e^- center-of-mass frame. On the contrary, the electric and the magnetic components of the Lorentz force provided by the oncoming bunch contribute equally, also up to the accuracy of the order of $1/\gamma$, to the focusing force that pinches the test bunch.

Let the density distribution of a bunch be decoupled for longitudinal and transverse directions:

$$n(r,z) = n_z(z)\,n_r(r) \quad , \tag{2.3}$$

where

$$n_z(z) = \begin{cases} \frac{1}{\sqrt{2\pi}\,\sigma_z}\,e^{-z^2/2\sigma_z^2} \quad , & -\infty < z < \infty \quad \text{(round gaussian)} \\ \frac{1}{2\sqrt{3}\,\sigma_z} \quad , & -\sqrt{3} < z < \sqrt{3} \quad \text{(uniform cylinder)} \end{cases} ,$$

$$n_r(r) = \begin{cases} \frac{1}{\sigma_r^2}\,e^{-r^2/2\sigma_r^2} \quad , & 0 \le r < \infty \quad \text{(round gaussian)} \\ \frac{1}{2\sigma_r^2} \quad , & 0 \le r \le 2\sigma_r \quad \text{(uniform cylinder)} \end{cases} .$$

The normalization coefficients are chosen such that $\int n_z(z)\,dz = 1$ and $\int n_r(r)\,r dr = 1$. The equation of motion for the test charge in a bunch at coordinate (r, z) is [6]

$$\frac{d^2r}{dt^2} = -\frac{4r_eN}{\gamma}\, f(r)\; n_z(-2t - z) \quad , \tag{2.4}$$

where

$$f(r) = \frac{1}{r}\int_0^r n_r(r')\; r'dr' \quad ,$$

$r_e = 2.818 \times 10^{-13}$ cm is the classical electron radius and $t = 0$ when the centroids of the two colliding bunches intercept. Figure 1 is a schematic diagram that shows definition of the coordinates. Consider, for example, uniform cylinder bunches. The above equation becomes

$$\frac{d^2r}{dt^2} + \frac{r_eN\, r}{2\sqrt{3}\gamma\sigma_r^2\sigma_z} = 0 \quad . \tag{2.5}$$

The solution is simply

$$r(t) = r_0 \cos\left[\left(\frac{r_eN}{2\sqrt{3}\gamma\sigma_r^2\sigma_z}\right)^{1/2} t + \phi\right] \quad , \tag{2.6}$$

where r_0 is the impact parameter of the test particle upon entering the target bunch and

$$\phi = \left(\frac{\sqrt{3}r_eN\sigma_z}{2\gamma\sigma_r^2}\right)^{1/2} \quad .$$

The deflection angle is therefore

$$\frac{dr}{dt} = -r_0\left(\frac{r_eN}{2\sqrt{3}\gamma\sigma_r^2\sigma_z}\right)^{1/2} \sin\left[\left(\frac{r_eN}{2\sqrt{3}\gamma\sigma_r^2\sigma_z}\right)^{1/2} t + \phi\right] \quad . \tag{2.7}$$

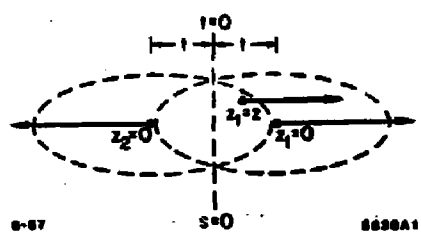

Fig. 1. Schematic diagram that defines the various coordinates of the two bunches during collision. For a test particle in bunch 1 at $z_1 = z$, the relative coordinate with respect to the center of bunch 2 is $z_2 = -2t - z$.

For a weak deflecting force, at the end of collision $t = \sqrt{3}\sigma_z$ we have

$$\frac{dr}{dt} \sim -\frac{r_e N}{\gamma \sigma_r^2} r_0 \quad . \tag{2.8}$$

When the two transverse dimensions have different distributions, i.e., $\sigma_x \neq \sigma_y$, this expression can be generalized to

$$\begin{aligned} \frac{dx}{dt} &\sim -\frac{2r_e N}{\gamma \sigma_x(\sigma_x + \sigma_y)} x_0 \quad , \\ \frac{dy}{dt} &\sim -\frac{2r_e N}{\gamma \sigma_y(\sigma_x + \sigma_y)} y_0 \quad . \end{aligned} \tag{2.9}$$

From ray optics the coefficients of eqs. (2.8) and (2.9) can be regarded as the inverse of the focal lengths.

We now define a dimensionless, Lorentz invariant parameter, called disruption parameter D [7], as a measure of the inverse of focal length in the units of bunch length σ_z in each of the transverse dimensions. The terminology dervived from the fact that during pinching, the beam emittances are severely disrupted. Explicitly,

$$\begin{aligned} D_x &= \frac{2r_e N \sigma_z}{\gamma \sigma_x(\sigma_x + \sigma_y)} \quad , \\ D_y &= \frac{2r_e N \sigma_z}{\gamma \sigma_y(\sigma_x + \sigma_y)} \quad . \end{aligned} \tag{2.10}$$

Let us further introduce the aspect ratio $R \equiv \sigma_x/\sigma_y \geq 1$, and call

$$D = D_y = \frac{r_e N \sigma_z}{\gamma \sigma_x \sigma_y} \left(\frac{2R}{1+R} \right) \quad . \tag{2.11}$$

Thus, $D_x = D/R$. For round beams $(R = 1) D_x = D_y$, and in the asymptotic limit for flat beams $(R \gg 1) D_x \approx 0$ and $D \approx 2r_e N \sigma_z / \gamma \sigma_x \sigma_y$.

For $D \ll 1$, the focusing force is weak enough that each bunch only converges to the axis after traversing the oncoming bunch; whereas for $D \gg 1$, the focal point lies well inside the oncoming bunch. Particles experiencing large values of D would then execute betatron oscillations during the course of collision.

To end this discussion we comment that in the regime where $D \not\ll 1$, the pinching of the bunches would causally affect the disruption for the remainder of the collision. One would therefore naturally think that the parameter D loses its meaning in the quantitative sense. It is fortuitous that actually D as defined does provide simple scaling laws as if the entire bunch has a well-defined focal length.

2.2 Disruption Angles

One important information for linear collider design is the expected disruption angle. Knowledge on the maximum disruption angle is essential to determine the aperture of the last element in a final focusing system such that it is able to avoid being showered by the debris from beam-beam collision.

In terms of D, eq. (2.7) can be rewritten as [6]

$$\frac{dr}{dt} = -\frac{r_0}{\sigma_z}\left(\frac{D}{2\sqrt{3}}\right)^{1/2} \sin\left[\left(\frac{D}{2\sqrt{3}}\right)^{1/2}\frac{t}{\sigma_z} + \phi\right] \quad . \tag{2.12}$$

For $D \ll 1$ and at the time when the test particle exists from the oncoming bunch

$$\frac{dr}{dt} \sim -\frac{r_0}{\sigma_z}\left(\frac{D}{2\sqrt{3}}\right)^{1/2}\left[\left(2\sqrt{3}D\right)^{1/2} + \frac{1}{3!}\left(2\sqrt{3}D\right)^{3/2} + \ldots\right] \quad , \quad D \ll 1 \quad . \tag{2.13}$$

For $D \gg 1$, at the time of exit from the oncoming bunch a test particle would have executed more than one cycle of betatron oscillation. Therefore, the sinusoidal function in eq. (2.12) is of order unity and

$$\frac{dr}{dt} \sim -\frac{r_0}{\sigma_z}\left(\frac{D}{2\sqrt{3}}\right)^{1/2} \quad , \quad D \gg 1 \quad . \tag{2.14}$$

The *rms* disruption angle $\theta_D^{rms} = \sqrt{\langle (dr/dt)^2 \rangle}$, and the maximum disruption angle θ_D^{max}, can be deduced from the above equations through $\sqrt{\langle r_0^2 \rangle}$ and r_0^{max}, respectively. It is obvious that in doing it this way the generic functional behavior of θ_D^{rms} and θ_D^{rms} are the same, i.e.,

$$\frac{\theta_D}{\theta_0} \sim \begin{cases} a + bD & , \quad D \ll 1 \quad , \\ \dfrac{c}{\sqrt{D}} & , \quad D \gg 1 \quad , \end{cases} \tag{2.15}$$

where a, b and c are some numerical coefficients which are different for θ_D^{rms} and θ_D^{max}, and θ_0 a reference angle defined as

$$\theta_0 = \frac{r_e N}{\gamma \sigma_r} \quad .$$

As was discussed earlier, during the collision both beams are continuously deformed due to the mutual pinching. Thus, for reliable estimations of these coefficients computer simulations are indispensable. Figure 2 shows θ_D^{max} and θ_D^{rms} as functions of D from computer simulations by Hollebeek and Minten [8, 9] and Yokoya [10]. The two sets of data are in reasonable agreement.

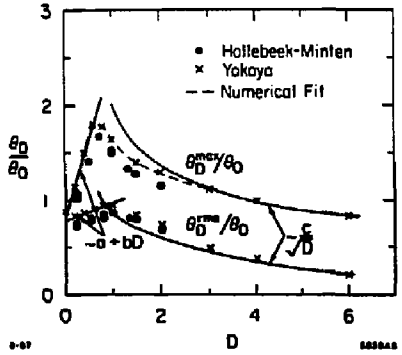

Fig. 2. The maximum and *rms* disruption angles as functions of D. The solid curves are from eqs. (2.16) and (2.17), and the dashed curve is from eq. (2.18).

From these curves we find

$$\frac{\theta_D^{max}}{\theta_0} \simeq \begin{cases} 0.087 + 1.57\,D\,, & D \ll 1\ , \\ \dfrac{1.84}{\sqrt{D}}\,, & D \gg 1\ . \end{cases} \tag{2.16}$$

And

$$\frac{\theta_D^{rms}}{\theta_0} \simeq \begin{cases} 0.78 + 0.20\,D\,, & D \ll 1\ , \\ \dfrac{0.67}{\sqrt{D}}\,, & D \gg 1\ . \end{cases} \tag{2.17}$$

These asymptotic behaviors are shown by solid curves in fig. 2. A different numerical fit which emperically matches the θ_D^{max} data for the entire range of D is given by Palmer [11]:

$$H_\theta = \frac{1}{\left(\frac{1}{1.2+50D^3}\right) + \left(0.06 + \frac{D}{3.38}\right)^{1/2}}\ . \tag{2.18}$$

This function is plotted as a dashed curve in the figure.

2.3 Luminosity Enhancement Factor

Since the bottom line of an accelerator design is the luminosity, the most important effect of disruption is the reduction of the effective cross sectional beam area, which causes enhancement of luminosity. As discussed above, this effect can be characterized by the luminosity enhancement factor $H_D = \mathcal{L}/\mathcal{L}_0$ where the luminosity is defined as

$$\mathcal{L} = 2N^2 f_r \int dx\,dy\,dz\,dt \cdot n(x,y,z-t) \cdot n(x,y,-z-t)\ . \tag{2.19}$$

$n(x,y,z-t)$ and $n(x,y,-z-t)$ are the local densities of the two beams at position (x,y,z) at time t.

To include the disruption effect we return to the equation of motion in eq. (2.4). The solution to the first order in D is [12]

$$r(t,s) = r_0 - \frac{4Nr_e}{\gamma} f(r_0)\, g(t,s) \quad , \tag{2.20}$$

where

$$g(t,s) = \int_{-\infty}^{t} dt_1 \int_{-\infty}^{t_1} dt_2\, n_z(-2t-s) = \int_{-\infty}^{t} dt_1\, (t-t_1)\, n_z(-2t-s) \quad .$$

Thus

$$r_0 \doteq r + \frac{4r_eN}{\gamma} f(r)\, g(t,s) \quad . \tag{2.21}$$

For our purpose we like to know the radial distribution function n_r at (t,s). This can be found by

$$\begin{aligned} n_r(t,s) &= n_r(r_0) \frac{d^2(r_0^2)}{d^2(r^2)} \\ &= n_r(r_0) \left[1 + \frac{4r_eN}{\gamma} g(t,s) \frac{1}{r}\frac{d}{dr}\left(r f(r)\right)\right] \\ &= \left[n_r(r) + \frac{dn_r(r)}{dr} \frac{4r_eN}{\gamma} f(r)\, g(t,s)\right] \cdot \left[1 + \frac{4r_eN}{\gamma} g(t,s)\, n_r(r)\right] \\ &\simeq n_r\left[1 + \frac{4r_eN}{\gamma}\left(\frac{1}{n_r}\frac{dn_r}{dr} f(r) + n_r\right) g(t,s)\right] \end{aligned} \tag{2.22}$$

With the above expression we can estimate the luminosity from eq. (2.19), which can also be expressed by the bunch coordinates introduced in fig. 1,

$$\begin{aligned} \mathcal{L} \propto \int & r dr\, ds_1 ds_2\, n_z(s_1) n_z(s_2)\, [n_r(r)]^2 \\ & \times \left[1 + \frac{4r_eN}{\gamma}\left(\frac{1}{n_r}\frac{dn_r}{dr} f(r) + n_r\right)\left(g(t,s_1) + g(t,s_2)\right)\right]_{t=\frac{s_1+s_2}{2}} \quad , \end{aligned} \tag{2.23}$$

where the leading term corresponds to the nominal luminosity $\mathcal{L}_0$. The integration over r can be carried out, which gives

$$\int_0^\infty r dr\, n_r^2 \left(\frac{1}{n_r}\frac{dn_r}{dr} f(r) + n_r\right) = \frac{1}{2}\int_0^\infty r dr\, n_r^2 \quad . \tag{2.24}$$

Thus the luminosity enhancement factor for small D is

$$H_{D1} \simeq 1 + \frac{4r_eN}{\gamma}\left[\frac{\frac{1}{2}\int n_r^3\, r dr}{\int n_r^2\, r dr}\right] \int ds_1 ds_2\, n_z(s_1) n_z(s_2) \left(g(t,s_1) + g(t,s_2)\right) \quad . \tag{2.25}$$

Since the two colliding bunches are symmetric, $g(t,z_1)$ and $g(t,z_2)$ contribute equally to H_D, where

$$g(t,z_1)\Big|_{t=\frac{z_1+z_2}{2}} = \int_{-\infty}^{t} dt_1 (t-t_1)\, n_z(-2t-z_1) = \frac{1}{4}\int_0^\infty r dr\, n_z(r+z_2) \quad . \tag{2.26}$$

Therefore

$$\begin{aligned} H_{D1} &\simeq 1+\frac{r_e N}{\gamma}\left[\frac{\int r dr\, n_r^3}{\int r dr\, n_r^2}\right] \int dz_1 dz_2\, n_z(z_1) n_z)\,(z_2) \int_0^\infty r dr\, n_z(r+z_2) \\ &= 1+\frac{r_e N}{\gamma}\left[\frac{\int r dr\, n_r^3}{\int r dr\, n_r^2}\right] \int_{-\infty}^{\infty} dz \int_0^\infty r dr\, n_z(z)\, n_z(r+z) \quad . \end{aligned} \tag{2.27}$$

Now we introduce normalised coordinates $\rho = r/\sigma_r$ and $\zeta = z/\sigma_z$. Then

$$H_{D1} \simeq 1+D\left[\frac{\int \rho d\rho\, n_\rho^3}{\int \rho d\rho\, n_\rho^2}\right] \int_{-\infty}^{\infty} d\zeta \int_0^\infty r dr\, n_z(\zeta)\, n_z(r+\zeta) \quad . \tag{2.28}$$

Plugging in distrubution functions from eq. (2.3), we obtain

$$H_{D1} \simeq \begin{cases} 1+\frac{2}{3\sqrt{\pi}} D+O(D^2) \quad , & \text{(round gaussian)} \quad , \\ \qquad\qquad D \ll 1 & \\ 1+\frac{1}{2\sqrt{3}} D+O(D^2) \quad , & \text{(uniform cylinder)} \quad . \end{cases} \tag{2.29}$$

So far the discussion has been limited to round beams. To extend the above expression to arbitrary values of R, it is more convenient to rewrite H_{D1} as an exponential function:

$$H_{D1} \simeq e^{2D/3\sqrt{\pi}} \quad , \qquad D \ll 1 \qquad \text{(round gaussian)} \quad . \tag{2.30}$$

Recall that for different aspect ratios D scales as $2R/(1+R)$ [cf., eq. (2.11)]. So naively one would tend to assume that $H_{D1}(R)$ varies as $\exp[2R/(1+R)]$, which is incorrect.

Notice that H_{D1} essentially comes from the relative change in beam spot sizes, i.e.,

$$H_{D1} = \frac{\sigma_x \sigma_y}{\bar{\sigma}_x \bar{\sigma}_y} \quad , \tag{2.30}$$

where $4\pi\bar{\sigma}_x\bar{\sigma}_y$ is the effective beam size. For round beams

$$\sqrt{H_{D1}} \equiv \frac{\sigma_r}{\bar{\sigma}_r} = e^{D/3\sqrt{\pi}} \quad , \quad D \ll 1 \quad . \tag{2.31}$$

Thus, for $R > 1$ we have [cf., eq. (2.11)]

$$\frac{\sigma_y}{\delta_y} = e^{D/3\sqrt{\pi}} \quad ; \quad \frac{\sigma_z}{\delta_z} = e^{D/3\sqrt{\pi}R} \quad , \quad D \ll 1 \quad . \tag{2.32}$$

Combining eqs. (2.32) and (2.30), we have

$$H_{D1}(R) = e^{(1+R)D/3\sqrt{\pi}R} \quad , \quad D \ll 1 \quad . \tag{2.33}$$

Now we replace $\exp[2D/3\sqrt{\pi}]$ by H_{D1}, then we obtain

$$H_{D1}(R) = H_{D1}^{(1+R)/2R} \quad . \tag{2.34}$$

This expression was first introduced by Amaldi [3].

Beyond the $D \ll 1$ limit, the disruption effect becomes very nonlinear and we lack analytic tools to derive luminosity enhancement factor rigorously. Computer simulations of H_D with negligible beamstrahlung have been studied by several authors. Figure 3 shows H_D as a function of D for round gaussian beams. The solid curve represents the original work of Hollebeek [7], where the initial beam emittance is zero. The dashed curve is from a recent study by Fawley and Lee [13] with $\epsilon_n = 6.7 \times 10^{-5}$ m-rad. Notice that the two curves are substantially different for $D \gtrsim 5$. While the Hollebeek data saturates at $H_D \simeq 6$, the Fawley–Lee result does not seem to saturate. Despite this disagreement, the curves are reasonably close to each other for $D < 1$, where our analytic formula in eq. (2.28) fits quite well.

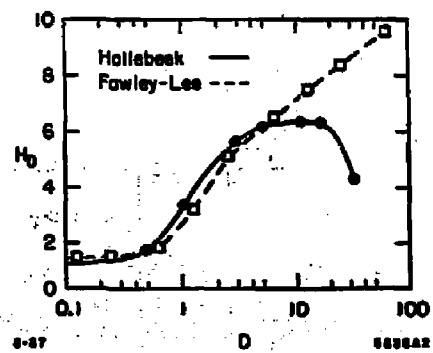

Fig. 3. The luminosity enhancement factor H_D as a function of D. The data are taken from the simulation results of Hollebeek, and Fawley and Lee.

2.4 The Effects Due to Initial Emittance

Effect on Luminosity Enhancement

In order to have a better assessment of the physical process that contributes to H_D beyond the limit of small D, we investigate the time evolution of H_D during beam-beam collision. For this purpose we single out the time dependence of $\mathcal{L}$ in eq. (2.19) and write

$$\mathcal{L} = \int_{-\infty}^{\infty} h(t)\, dt \quad . \tag{2.35}$$

The function $h(t)$ is thus the "differential" luminosity in time. A normalized $h(t)$ (i.e., $h(t)/\mathcal{L}$) was simulationed by Chen and Yokoya [12]. The histograms for $D \leq 1$ are shown in fig. 4.

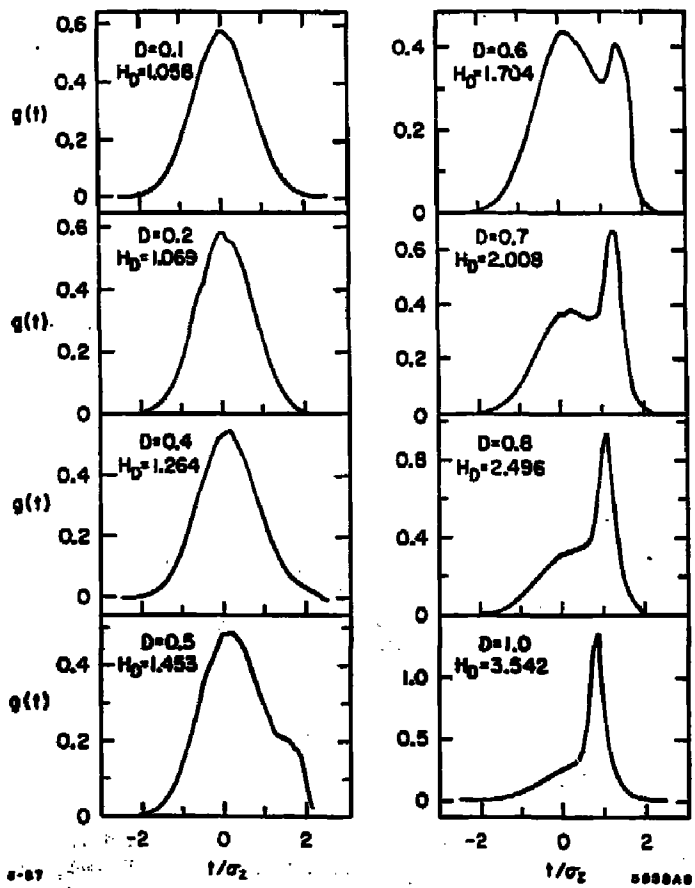

Fig. 4. Computer simulations by Chen and Yokoya on the time evolution of luminosity for different values of D.

From the figures we see that when D is very small, e.g., $D \lesssim 0.5$, the histogram follows essentially as the square of bunch-current distribution, which in our case is gaussian. In this region of D the enhancement of luminosity occurs through the overall demagnification of the beam cross sections, as discussed in the previous section, where H_{D1} in eq. (2.30) agrees reasonably well with the values shown in the first four diagrams in fig. 4, as it should.

When $D \sim 0.5$, a second peak appears. This is explained to be caused by particles at certain radius (not the entire cross section) focused on beam axis within the oncoming bunch. At $D = 0.5$, this peak occurs at $t = 1.5\sigma_z$. The peak grows as D gets larger, and eventually becomes the dominant source for the luminosity enhancement by $D \sim 1.0$. Notice also that the location of the second peak shifts gradually to the left when D gets larger, where the stronger disruption induces the phenomena to occur earlier in time. The steepness of this peak suggests that tiny time steps are required in simulation.

Since the second peak is believed to be caused by particles focused on axis, where very high density would occur within a tiny volume, we need to fine tune the radial mesh sizes in order to avoid underestimating the luminosity at the focal point. Figure 5 shows H_D as a function of $\ell n(1/dr)$, where dr is the radial mesh size in units of σ_r in each of the computer runs. The simulation was done [12] by assuming zero initial emittance for $D = 1$ and 4. It is seen that H_D scales roughly linearly as $\ell n(1/dr)$, which is clearly divergent. This implies that the functional behavior of H_D with zero beam emittance is very subtle. A finite value of H_D could be obtained by a randomly chosen mesh size (or the number of macroparticles) in a simulation with zero emittance, but the result would not be numerically stable.

The symptom for zero emittance beams arises because all particles enter the oncoming bunch in parallel, thus those with the same impact parameter would be focused to a single point. For beams with nonzero initial emittance there would be a smearing effect that this singular behavior

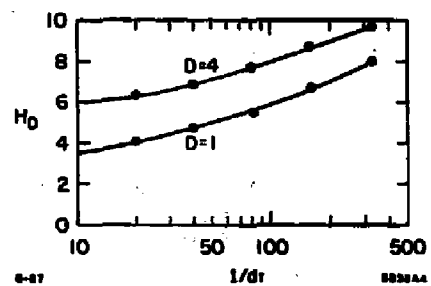

Fig. 5. H_D as a function of the inverse of the radial mesh size, $1/dr$, in computer simulations for $D = 1$ and 4. The initial emittance is zero.

can never occur. Let us introduce a Lorentz invariant, dimensionless parameter A that manifests the beam emittance for fixed σ_x and σ_y:

$$A = \frac{\sigma_x}{\beta^*} = \frac{\epsilon_n D}{r_e N} \quad , \tag{2.36}$$

where β^* is the β-function at the interaction point. Figure 6 shows H_D with three different values of A ($A = 0.1$, 0.2, and 0.4), the simulations use the computer code ABEL developed by Yokoya [14]. As expected, smaller A gives larger values of H_D. Furthermore, from the figure we find that

$$H_D(A = .01) - H_D(A = 0.2) \simeq H_D(A = 0.2) - H_D(A = 0.4) \quad , \tag{2.37}$$

for a given value of D, but the separation increases roughly quadratically. This suggests that the part of the luminosity enhancement arising from the second peaks in fig. 4 scales as

$$H_{D2} \propto \left[\ln\left(\frac{D}{A}\right)\right]^2 \quad . \tag{2.38}$$

From fig. 6 we deduce that

$$H_D \simeq \lambda_1 + \lambda_2 \left[\ln\left(\frac{D}{A}\right)\right]^2 \quad , \quad D \gg 1 \quad , \tag{2.39}$$

where $\lambda_1 \simeq 1.6$ and $\lambda_2 \simeq 0.43$.

Putting everything together, the overall luminosity enhancement is now

$$H_D = \begin{cases} H_{D1} \simeq 1 + \frac{2}{3\sqrt{\pi}} D \quad , & 0 < D \lesssim 0.5 \quad , \\ H_{D1} + H_{D2} \simeq 1 + \frac{2}{3\sqrt{\pi}} D + 0.43 \left[\ln\left(\frac{D}{A}\right)\right]^2 \quad , & 0.5 \lesssim D \lesssim 2 \quad , \\ H_{D1}^{\max} + H_{D2} \simeq 1.6 + 0.43 \left[\ln\left(\frac{D}{A}\right)\right]^2 \quad , & 2 \lesssim D \lesssim 100 \quad , \end{cases} \tag{2.40}$$

where λ_1 has been identified to be the saturation of H_{D1} at $D \gtrsim 2$, at which value the pinching has induced roughly half a cycle of plasma oscillation [7]. The nonsaturation of H_D's in fig. 6 are characteristically different from that of Hollebeek in fig. 3, but show similar tendency as that of Fawley and Lee.

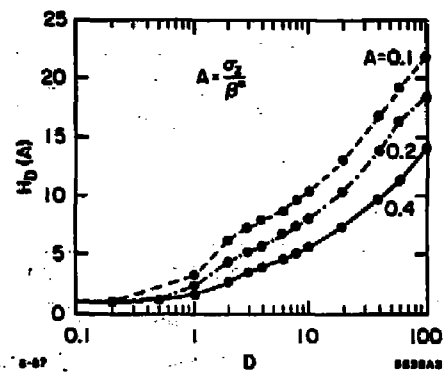

Fig. 6. Luminosity enhancement factor H_D with different values of A simulated by Chen and Yokoya.

Effects on Disruption Angles

With the drastic impact on luminosity enhancement in mind, it is natural to ask whether the initial emittance also makes large influence on the disruption angles described in sec. 2.2. Simulations are done by Chen and Yokoya [12] in this respect. Figure 7 shows θ_D^{max} and θ_D^{rms} in the units of σ_x/σ_z. Again, $A = 0.1$, 0.2, and 0.4 are used to find the sensitivity of the angles on A. The data in the figure evidently show that the disruption angles are asymptotically independent of A. Thus all the statements in sec. 2.2 remain unchanged.

The fact that the disruption angles are independent of A can be understood as follows: While luminosity comes from multiplying local densities of both colliding bunches, disruption angles depend only on the integrated density of the oncoming bunch (through Gauss's law). Under this light the sharp focus of the like particles on axis would have no effect on disruption. Furthermore, the Lorentz force provided by the oncoming bunch at any radius $r > 0$ would be the same around the focal point independent of whether the focus is sharp or blurry.

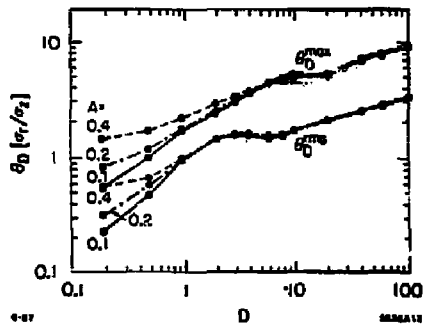

Fig. 7. Disruption angles with different values of A simulated by Chen and Yokoya. θ_D's are in the units of σ_x/σ_z.

3. BEAMSTRAHLUNG WITH NEGLIGIBLE DISRUPTION

In this section we first review the novel characters of beamstrahlung assuming no bunch deformations. This serves as an introduction to the more specific discussions following that. To discuss radiation, we take an iterative approach. First we examine the problem with semi-uniform field approximation that is suitable for long bunches, from which a beamstrahlung reduction factor H_{T1} is obtained. Next we include the fact that the field strength in a bunch is actually varying along the trajectory of a radiating particle. This results in a second beamstrahlung reduction factor H_{T2} when the bunch is short.

With efforts in recent years, the understanding of the subject is rapidly maturing, though with a wide spectrum of appoaches to the problem. To be self-consistent in our treatment it is difficult, if not impossible, to review various different calculations in detail. Instead we will only mention each individual contribution in passing wherever is appropriate.

3.1 The Nature of Beamstrahlung

Collective Fields from Discrete Scattering Centers

In the laboratory frame (also the center-of-mass frame in our case) of a linear collider, an electron encountering a positron with an impact parameter b would have an effective interaction time $\Delta t_1 \sim b/\gamma$ due to the fact that the fields associated with relativistic particles span about an opening angle $\Delta\theta \sim 1/\gamma$. In turn, the corresponding effective distance of traverse through the fields of the oncoming particle is

$$\ell_1 = t_1 \sim \frac{b}{\gamma} \quad . \tag{3.1}$$

Consider an electron encountering the entire flux of the oncoming positron bunch. The flux is roughly

$$\frac{N}{\sigma_z} \equiv \frac{1}{\ell_2} \quad , \tag{3.2}$$

where ℓ_2 is the mean longitudinal separation of target particles. The target beam is considered to be dense if $\ell_1 \gg \ell_2$. Taking a typical value of impact parameters to be one standard deviation in the transverse direction, i.e., $b \sim \sigma_r$, the condition for a dense beam translates into

$$\frac{N\sigma_r}{\gamma\sigma_z} \gg 1 \quad . \tag{3.3}$$

In this case the background field provided by the particles in the oncoming bunch is continuous. (See fig. 8.) For example, the Stanford Linear Collider (SLC) beam parameters are $\gamma = 1 \times 10^5$, number of particles per bunch $N = 5 \times 10^{10}$, $\sigma_z \sim 1$ mm, $\sigma_r \sim 1$ μm at the interaction point. Thus $N\sigma_r/\gamma\sigma_z \sim 500 \gg 1$, and the beam is *dense*.

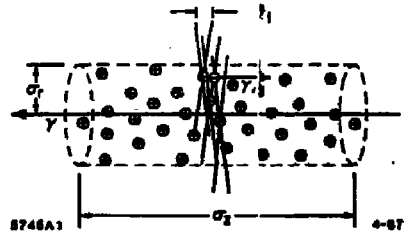

Fig. 8. A schematic diagram for a "dense" beam.

A beam is said to be *dilute* if $\ell_2 \ll \ell_1$, or

$$\frac{N\sigma_r}{\gamma\sigma_z} \ll 1 \quad . \tag{3.4}$$

In this case the background field becomes discrete and the test particle would see the granularity of the target bunch. (See fig. 9.) For example, in the conceptual accelerator of 5 TeV+5TeV discussed by Richter [15], and refined by Himel and Siegrest [16], $\gamma = 1 \times 10^7$, $N = 1.2 \times 10^8$, $\sigma_z = 0.4$ μm and $\sigma_r = 2.5$ Å, we have $N\sigma_r/\gamma\sigma_z \sim 0.0075 \ll 1$. The beam is therefore quite *dilute*.

In one version of the CLIC parameters [17], where $\gamma = 2 \times 10^6$, $N = 5.4 \times 10^9$, $\sigma_z = 0.5$ mm and $\sigma_r = 65$ mm, we find $N\sigma_r/\gamma\sigma_z \sim 0.35 \lesssim 1$. In this case the beam is only marginally dilute.

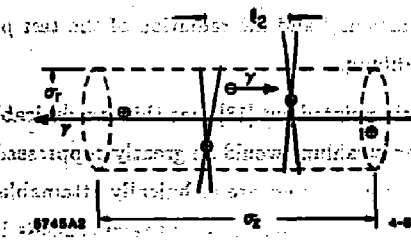

Fig. 9. A schematic diagram for a "dilute" beam.

The length scales ℓ_1 and ℓ_2 introduced above arise from kinematic origins. Now we introduce one more length scale, the radiation formation length ℓ_R, which arises from dynamic origin. The radiation formation length is the length which an electron (or a positron) must travel for a photon to be emitted within an open cone with angle $\sim 1/\gamma$. (More detailed discussion on ℓ_R is given in sec. 3.2.2.) Together with the bunch length σ_z, the four length scales comprise eight possible situations, where ℓ_1, $\ell_2 < \sigma_z$ by definition. Among the eight arrangements, the cases $\ell_R < \ell_1 < \ell_2 < \sigma_z$, $\ell_R < \ell_2 < \ell_1 < \sigma_z$ and $\ell_1 < \ell_R < \ell_2 < \sigma_z$ assume a chain of close encounters between the test electron and the positrons where each deflection causes a bending angle of more than $\sim 1/\gamma$, which is very unlikely. The remaining five cases can be categorized into the following:

a. $\ell_2 < \ell_R < \ell_1 < \sigma_z$: The bunch is so dense that the test particle would be bent severely and quickly lose all its energy. This is a situation where the accelerator designers would definitely want to avoid.

b. $\ell_2 < \ell_1 < \ell_R < \sigma_z$ (dense beam) and $\ell_1 < \ell_2 < \ell_R < \sigma_z$ (dilute beam): In this regime the test electron interacts with the macroscopic fields collected from positrons within the range of ℓ_R. For dense beams, the collective fields within ℓ_R are smooth. The radiation in this case is similar to the familiar "synchrotron radiation."

   For dilute beams, the interaction with the test particle is still collective, but the discrete fields would act somewhat like "undulators" with mean periodicity $\sim \ell_2$. These "undulators" would then induce ripples onto a smooth trajectory associated with the mean charge distribution of the target. This would potentially introduce extra radiation. We will discuss this point in more details later.

   It occurs that almost all linear collider beam parameters that people discussed are in this category. So the rest of this section will be devoted primarily to this case.

c. $\ell_1 < \ell_2 < \sigma_z < \ell_R$ and $\ell_2 < \ell_1 < \sigma_z < \ell_R$: This corresponds to the condition where the bunch is ultrashort. In this regime the whole target bunch acts like a "positron nucleus," and the radiation of the test particle is more like that in bremsstrahlung.

   It has been recently pointed out [18] that this is a desirable beam parameter regime where beamstrahlung would be greatly suppressed. But it is unclear whether such beam parameters are technically attainable and whether they will conflict with other stringent physical requirements in a linear collider. We therefore view it as an interesting option which requires further studies.

Presence of Both Electric and Magnetic Fields

Unlike a permanent magnet, in beamstrahlung the target bunch presents both electric and magnetic fields in the e^+e^- center-of-mass frame, whereas in the rest frame of the target bunch there is only E–field. In fact, in our case $(|\vec{E}|^2 - |\vec{B}|^2)/|\vec{E}|^2 \sim 1/\gamma^2 \gtrsim 0$, and one can never find a frame where there is only B–field.

Facing this fact, two different approaches have been taken. One can either work in the rest frame of the target bunch, which is what Blankenbecler and Drell [19] and Jacob and Wu [20] did, or work in the center-of-mass frame and assume the Lorentz force due to $\vec{E}$ and $\vec{B}$ to be equal. This second approach has been taken by Himel and Siegrist [16], Noble [21], Yokoya [14, 22] and Chen [23].

Quantum mechanically, in principle, an electron interacts with $\vec{E}$ and $\vec{B}$ very differently. For example, while an electron would execute a circular orbit in a transverse uniform magnetic field, it would instead have an open orbit when traversing a transverse uniform electric field. (See fig. 10.) This difference is the genesis of the well-known historical issue called Klein paradox [24] where spontaneous e^+e^- pair creation is possible when the electron is accelerated in a strong E–field.

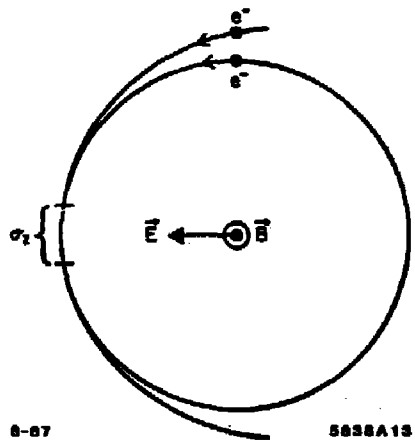

Fig. 10. Closed and open trajectories of an electron under $\vec{B}$ and $\vec{E}$ fields, respectively. For $|\vec{B}| = |\vec{E}|$ the two trajectories largely overlap around the turning point.

However, it is shown by Chen and Noble [25] that beamstrahlung actually occurs within a very short distance $\sim \sigma_z$ around the turning point, where there is no essential distinction between the two possible trajectories. (See the overlapping section in fig. 10 indicated by σ_z.) More specifically, when the electron momentum which is transverse to $\vec{E}$ is much larger than the rest mass, i.e., $p_\perp \gg m$, and when $e|\vec{E}|/m \ll 1$, the radiation rates are the same from $\vec{E}$ and $\vec{B}$ given equivalent strengths. We will base the rest of our discussion of beamstrahlung on this argument.

Finite Extents of the Fields

Unlike the *bona fide* synchrotron radiation where the entire closed orbit of an electron is embedded in a uniform magnetic field, in beamstrahlung the field has finite extents. The strength of the EM field is proportional to the bunch current, which typically varies as a gaussian function. Very often an equivalent uniform distribution with total length $L = 2\sqrt{3}\sigma_z$ are invoked [cf., eq. (2.3)] for the sake of mathematical simplicity. A schematic drawing is shown in fig. 11. In the transverse direction, the local field strength also varies.

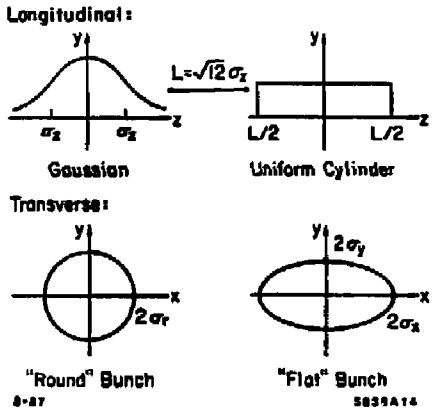

Fig. 11. Schematic diagrams of charge distributions in longitudinal and transverse directions.

For a round beam (i.e., $R = 1$) with a bi-gaussian charge distribution

$$n_{R=1}(r,z) = \frac{1}{(2\pi)^{3/2}\sigma_r^2\sigma_z} e^{-r^2/2\sigma_r^2} e^{-z^2/2\sigma_z^2} \quad , \tag{3.5}$$

the corresponding field strength is

$$|\vec{E}|_{R=1} \simeq |\vec{B}|_{R=1} = \frac{eN}{\sqrt{2\pi}\sigma_z} \cdot \frac{1}{r}\left[1 - e^{-r^2/2\sigma_r^2}\right] \cdot e^{-z^2/2\sigma_z^2} \quad , \tag{3.6}$$

where $\vec{E}$ is in the radial direction and $\vec{B}$ is in the azimuthal direction. In the more general case of a flat beam (i.e., $R < 1$) with a tri-gaussian charge distribution

$$n_{R<1}(x,y,z) = \frac{1}{(2\pi)^{3/2}\sigma_x\sigma_y\sigma_z} e^{-x^2/2\sigma_x^2} e^{-y^2/2\sigma_y^2} e^{-z^2/2\sigma_z^2} \quad , \tag{3.7}$$

the $\vec{E}$-field is generally not pointing to the radial direction. The field strength is [26]

$$|\vec{E}|_{R>1} \simeq |\vec{B}|_{R>1} = \frac{eN}{\sigma_y \sigma_z} \frac{e^{-x^2/2\sigma_x^2}}{\sqrt{R^2-1}} \cdot \left| w\left(\frac{x+iy}{\sqrt{2(R^2-1)}\sigma_y}\right) - \exp\left\{-\left[\frac{x^2}{2\sigma_x^2}+\frac{y^2}{2\sigma_y^2}\right]\right\} w\left(\frac{x/R+iRy}{\sqrt{2(R^2-1)}\sigma_y}\right)\right| \quad , \tag{3.8}$$

where $w(\zeta)$'s are complex error functions.

From eqs. (3.6) and (3.8) it is clear that the fields in a bunch extend only within a finite space with strengths varying from point to point. We like to stress, however, that their longitudinal variation follows exactly the distribution of the bunch charge.

3.2 Synchrotron Radiation in a Semi-Uniform Field

Baier-Katkov Approach

Our starting point is the Baier-Katkov method of radiation calculation [27]. A similar method had been used earlier by Schwinger [28]. The method is based on the realization that when the radiating particle is ultrarelativistic, its radiation in a magnetic field is a quasi-classical problem. By that we mean the motion of an electron becomes more and more "classical" as its energy increases that it makes sense to describe the particle by its trajectory. The radiation is therefore viewed as induced by the bending of the trajectory. The only role that quantum physics plays is the noncommutativity between the electron field and the photon field, and the conservation of initial and final energies in a discrete manner. The general expression of radiation intensity (in the Coulomb gauge) is

$$I = \alpha \int \frac{d^3k}{(2\pi)^2} \langle i| \int dt_1 \int dt_2 \, e^{i\omega(t_1-t_2)} M^* \, (t_2) \, M \, (t_1) \, |f\rangle \quad , \tag{3.9}$$

where $\alpha = 1/137$ is the fine structure constant, $(\omega, \vec{k})$ the four-momentum of the photon, $\langle i|$, $\langle f|$ the initial and final states of electron, respectively, and M the transition matrix. To the accuracy of the order of $1/\gamma$, Baier and Katkov show that the phase factor from M^*M

$$e^{i\vec{k}\cdot\vec{r}(t_2)} e^{i\vec{k}\cdot\vec{r}(t_1)} = \exp\left\{i\left[\omega\tau + \frac{\mathcal{H}}{\mathcal{H}-\omega}\left(\vec{k}\cdot(\vec{r}(t_2)-\vec{r}(t_1)) - \omega\tau\right)\right]\right\} \quad , \tag{3.10}$$

where $\tau \equiv t_2 - t_1$ and $t = t_1 + t_2$, commutes with both the Hamiltonian $\mathcal{H}$ and the electron momentum $\vec{p}$. After summing over the spins of the final electron and polarizations of the photon, and averaging over the initial electron spins, the radiation intensity can be written as

$$\frac{dI}{dt} = \frac{\alpha}{(2\pi)^2} \int d^3k \int_{-\infty}^{\infty} d\tau \, G(\vec{v}(t_1), \vec{v}(t_2)) \exp\left\{ i \left[\omega\tau + \frac{\mathcal{E}}{\mathcal{E}'} \left(\vec{k} \cdot (\vec{r}(t_2) - \vec{r}(t_1)) - \omega\tau \right) \right] \right\} \quad , \tag{3.11}$$

where $\mathcal{E}$ and $\mathcal{E}'$ are the initial and final energies of the electron and

$$G(\vec{v}(t_1), \vec{v}(t_2)) = \frac{1}{4} \left[\left(1 + \frac{\mathcal{E}}{\mathcal{E}'} \right)^2 (\vec{v}(t_2) \cdot \vec{v}(t_1) - 1) + \left(\frac{\omega}{\mathcal{E}'} \right)^2 \left(\vec{v}(t_2) \cdot \vec{v}(t_1) - 1 + \frac{2}{\gamma^2} \right) \right] \quad . \tag{3.12}$$

From now on we will simplify the notations by designating $\vec{v}_1$ and $\vec{v}_2$ for $\vec{v}(t_1)$ and $\vec{v}(t_2)$, respectively. Similar notations apply for $\vec{r}(t)$. It is observed that the dominant contribution of the τ integration in eq. (3.11) comes from the value at $\dot{v}\tau \sim 1/\gamma$. This corresponds to the situation where the electron position vector has swept through an angle $1/\gamma$, or correspondingly the outcoming photon lies within an open cone of angle $1/\gamma$. We shall call this period of time the radiation formation time τ, and the corresponding distance of travel by the electron the radiation formation length, ℓ_R. Since $1/\gamma \ll 1$ we can Taylor expand $\vec{v}_2$ and $\vec{r}_2$ in terms of $\vec{v}_1$ and $\vec{r}_1$:

$$\begin{aligned} \vec{v}_1 \cdot \vec{v}_2 &= \vec{v}_1 \cdot \left[\vec{v}_1 + \dot{\vec{v}}_1 \tau + \frac{1}{2} \ddot{\vec{v}}_1 \tau^2 + \frac{1}{6} \dddot{\vec{v}}_1 \tau^3 + \ldots \right] \quad , \\ \vec{k} \cdot (\vec{r}_2 - \vec{r}_1) &= \vec{k} \cdot \left[\vec{v}_1 \tau + \frac{1}{2} \dot{\vec{v}}_1 \tau^2 + \frac{1}{6} \ddot{\vec{v}}_1 \tau^3 + \ldots \right] \quad . \end{aligned} \tag{3.13}$$

In their paper [27] Baier and Katkov truncated the expansion at $\ddot{\vec{v}}_1 \tau^2$, thus the assumption was

$$\frac{(1/6)|\dddot{\vec{v}}_1|\tau^3}{(1/2)|\ddot{\vec{v}}_1|\tau^2} \ll 1 \quad . \tag{3.14}$$

Since $B \propto \dot{v}$ in a magnetic field, and $\vec{v}^2 =$ constant, we have $\vec{v} \cdot \dot{\vec{v}} = 0$. Taking time derivatives successively, we have

$$\vec{v} \cdot \ddot{\vec{v}} = -\dot{\vec{v}} \cdot \dot{\vec{v}} \quad , \quad \vec{v} \cdot \dddot{\vec{v}} = -3\dot{\vec{v}} \cdot \ddot{\vec{v}} \quad , \text{ etc.} \tag{3.15}$$

Using these relations the assumption can be translated into $\dot{B}\tau/B \ll 1$. Now we define a dimensionless, Lorentz invariant parameter Υ:

$$\Upsilon = \gamma \cdot \frac{B}{B_c} = \frac{\dot{v}\gamma^3}{\mathcal{E}} \quad , \tag{3.16}$$

where $B_c = m^2c^3/e\hbar \simeq 4.4 \times 10^{13}$ Gauss is the Schwinger critical field strength [28]. The radiation intensity for electrons in a semi-uniform field satisfying $\dot{B}\tau/B \ll 1$ can then be obtained in terms of Υ:

$$\frac{dI_0}{dt} = \begin{cases} \frac{2}{3}\alpha m^2 \mathrm{T}^2 \left(1 - \frac{55\sqrt{3}}{16}\mathrm{T} + 48\mathrm{T}^2 + \ldots\right) & , \quad \mathrm{T} \ll 1 \quad . \\ \frac{32}{245}\Gamma\left(\frac{2}{3}\right) \alpha m^2 (3\mathrm{T})^{2/3} + \ldots & , \quad \mathrm{T} \gg 1 \quad . \end{cases} \tag{3.17}$$

In the above equation the expression for $\mathrm{T} \ll 1$ is the well-known formula for classical synchrotron radiation, including the leading quantum correction first derived by Schwinger [28], and independently by Sokolov, Klepikov and Ternov [29], and higher terms in T. The expression for $\mathrm{T} \gg 1$ corresponds to the synchrotron radiation in the extreme quantum limit studied by many people, but in this article we will simply call it Sokolov–Ternov formula [30]. The fact that Baier and Katkov reproduce these formulas in a straightforward manner and generalise them from strictly uniform fields to semi-uniform fields suggests the power of this method.

Formation Length and Granularity

Let us now digress from the above results. The radiation intensity in eq. (3.17) is the *total* intensity from all possible frequencies. If we look for the power spectrum $P(\omega)$, defined as

$$\frac{dI}{dt} = \int_0^\infty P(\omega)\, d\omega \quad , \tag{3.18}$$

it is known that in the classical limit it scales like

$$P(\omega) \sim \begin{cases} \omega^{1/3} & , \quad \omega \lesssim \omega_c \quad , \\ \frac{\omega}{\omega_c}\, e^{-\omega/\omega_c} & , \quad \omega \gtrsim \omega_c \quad . \end{cases} \tag{3.19}$$

The critical frequency ω_c is defined such that the total radiation intensity contributed from $\omega \leq \omega_c$ is equal to that from $\omega \geq \omega_c$. Notice, however, that higher frequency photons weighted more in terms of intensity. Therefore, the spectrum beyond ω_c does not cover as large an area as that below ω_c. In fact $P(\omega)$ diminishes exponentially beyond ω_c. For a uniform magnetic field, an electron would execute a closed orbit with radius ρ. The critical frequency is related to ρ by

$$\omega_c = \frac{3}{2}\frac{\gamma^3}{\rho} \quad , \tag{3.20}$$

where two powers of γ comes from Doppler shift due to the fact that the relativistic radiating particle co-moves with the emitted photon. The *rms* opening angle of emitted photons at this frequency is $\sim 1/\gamma$. For frequencies above or below ω_c, the opening angle varies as

$$\theta_{rad} \sim \begin{cases} \frac{1}{\gamma}\left(\frac{\omega_c}{\omega}\right)^{1/3} & , \quad \omega \lesssim \omega_c \quad , \\ \frac{1}{\gamma}\left(\frac{\omega_c}{\omega}\right)^{1/2} & , \quad \omega \gtrsim \omega_c \quad . \end{cases} \tag{3.21}$$

We shall therefore call the corresponding distance of travel of the electron the radiation formation length $\ell_R(\omega)$

$$\ell_R(\omega) \equiv \begin{cases} \frac{\rho}{\gamma}\left(\frac{\omega_c}{\omega}\right)^{1/3} & , \ \omega \lesssim \omega_c \ , \\ \frac{\rho}{\gamma}\left(\frac{\omega_c}{\omega}\right)^{1/2} & , \ \omega \gtrsim \omega_c \ . \end{cases} \tag{3.22}$$

The parameter T defined in eq. (3.16) can now be related to ω_c (and therefore ℓ_R). From Lorents force $|\vec{F}| = e\,|\vec{B}| = \gamma m/\rho$, we have

$$\mathrm{T} = \gamma \frac{B}{B_c} = \frac{\gamma^2 \lambda\!\!\!^{-}_c}{\rho} = \frac{2}{3}\frac{\omega_c}{\mathcal{E}} \ , \tag{3.23}$$

where $\lambda\!\!\!^{-}_c = \hbar/mc \simeq 3.8 \times 10^{-11}$ cm is the Compton wavelength. When $\mathrm{T} \ll 1$, we find $\omega_c \ll \mathcal{E}$. In this limit the typical energy of photons is much smaller than the electron energy and the entire power spectrum of eq. (3.19) is observable. On the other hand, when $\mathrm{T} \gg 1$, or $\mathcal{E} \ll \omega_c$, the spectrum beyond $\omega = \mathcal{E}$ is kinematically forbidden. So in the quantum limit, only the *infrared* region of the assumed classical spectrum is observable, which scales as $P(\omega) \sim \omega^{1/3}$ up to $\omega \simeq \mathcal{E}$ and ω_c is certainly not to be seen.

Panofsky [31] argued that in a dilute beam, the possible ripples that superposed to the smooth trajectory would induce additional radiation analogous to the undulator effect. This radiation introduces a broad spike with mean frequency associated with the mean particle separation ℓ_2,

$$\omega_d \simeq \frac{2\pi}{\ell_2}\gamma^2 \ . \tag{3.24}$$

Since $\omega_c \sim 2\pi\gamma^3/\ell_R$, and $\ell_R > \ell_2$, we have $\omega_d > \omega_c$. It is thus clear that this possible granularity effect is observable only when $\mathrm{T} \ll 1$. Beyond the classical regime ω_d, as well as ω_c, is kinematically forbidden. This means that even though the fields are physically discrete in a dilute beam, the radiating particle only responds to the mean of the field variation. This argument has been explicitly confirmed by Blankenbecler and Drell [19]. In their calculation, the electrostatic potential of each individual target particle (in the rest frame) was summed up and the fluctuation is shown to be logarithmically unimportant.

There is, however, an additional radiation effect due to the corpuscular nature of the target which is independent of whether the beam is dilute or dense. This corresponds to the bremsstrahlung from the individual scattering between the test electron and the positrons (and vice versa) recently calculated by Baier, Katkov and Strakhovenko [32]. The difference between this effect and the normal bremsstrahlung is that the former is strongly influenced by the macroscopic background field that we have been discussing so far. This subject, however, lies beyond the scope of our article, which deals with the radiation from a particle interacting with the bulk part of the target field only.

3.3 Synchrotron Radiation in a Varying Field

Head–Tail Symmetry and Gaussian Correction

Consider a magnetic field that points to the direction transverse to the axis where an electron enters, and its strength that varies along the axis. Let $t = 0$ when the electron passes the geometric center of the field. We are interested in the case where the field variation is such that $B(t)$ is an even function in t, which is also called head-tail symmetric. Since from Lorentz force $\dot{v} \propto B(t)$, we see that $\vec{v} \propto \dot{B}(t)$ is an odd function in t. Therefore, in the study of radiation from a head-tail symmetric inhomogeneous magnetic field, the terms linear in $\vec{v}$ would vanish when integrating over t. This means the leading correction term is of the order $\vec{v}^3$. We should thus retain the Taylor expansion in the integrand G up to the term $\vec{v}_1 \cdot \dddot{\vec{v}}_1 \tau^4$ where the recurrence relation

$$\vec{v} \cdot \dddot{\vec{v}} = -3\ddot{\vec{v}} \cdot \ddot{\vec{v}} - 4\dot{\vec{v}} \cdot \dddot{\vec{v}} \quad , \tag{3.25}$$

which is obtained from one more derivative on eq. (3.15), links the term with $\ddot{\vec{v}} \cdot \ddot{\vec{v}}$ and $\dot{\vec{v}} \cdot \dddot{\vec{v}}$ where both are even functions in time.

As for the phase, retaining terms up to $\ddot{\vec{v}} \cdot \ddot{\vec{v}}$ we have

$$\exp\left\{i\left[\omega\tau + \frac{\mathcal{E}}{\mathcal{E}'}\left(\vec{k}\cdot(\vec{r}_2 - \vec{r}_1) - \omega\tau\right)\right]\right\} = \exp\left\{-i\left(\Phi_0 + \Phi_1\right)\right\} \quad , \tag{3.26}$$

where

$$\Phi_0 = u\mathcal{E}\tau\left[1 - \hat{n}\cdot\vec{v} - \frac{1}{2}\hat{n}\cdot\dot{\vec{v}}\tau + \frac{1}{6}\ddot{\vec{v}}\cdot\ddot{\vec{v}}\tau^2\right] \quad ,$$

and $u \equiv \omega/\mathcal{E}'$, $\hat{n} \equiv \vec{k}/\omega$, is the phase angle that gives rise to eq. (3.17) in the previous section, and

$$\Phi_1 = u\mathcal{E}\tau\left[\frac{1}{8}\frac{\dot{\vec{v}}\cdot\ddot{\vec{v}}}{\vec{v}^3}\vec{v}^3\tau^3 + \frac{1}{120}\left(3\frac{\ddot{\vec{v}}\cdot\ddot{\vec{v}}}{\vec{v}^4} + 4\frac{\dot{\vec{v}}\cdot\dddot{\vec{v}}}{\vec{v}^4}\right)\vec{v}^4\tau^4\right]$$

is the additional phase that we retain. Notice that in Φ_1 and the last term in Φ_0 we had made the approximation of replacing $\hat{n}$ by $\vec{v}$.

We further assume that $\Phi_1 \ll 1$, which is usually satisfied if only $u \not\gg 1$, or the final energy of the electron $\mathcal{E}' \gg m$. This does not introduce extra assumption since the Baier–Katkov method has already assumed relativistic electron before and after emitting the photon. Therefore we make the following approximation:

$$\exp\left\{-i\left(\Phi_0 + \Phi_1\right)\right\} \simeq \left(1 - i\Phi_1\right)\exp\left\{-i\Phi_0\right\} \quad . \tag{3.27}$$

Retaining terms to the same order in the integrand G, and combining with eq. (3.27), we find the integrand to be

$$G = G_0 + G_1 + G_2 \quad , \tag{3.28}$$

where

$$G_0 = -\frac{1}{\gamma^3}(1+u) - \frac{1}{2}\left(1+u+\frac{u^2}{2}\right)\dot{v}^2\tau^2$$

is the part that reproduces the Sokolov–Ternov formula, $G_1 \propto \dot{B}\tau/B$ is an odd function in time and would give zero contribution for head-tail symmetric fields, and G_2 is

$$\begin{aligned} G_2 = &-\left(1+u+\frac{u^2}{2}\right)\left(\frac{1}{8}\frac{\dot{B}^2}{B^4}+\frac{1}{6}\frac{\ddot{B}}{B^3}\right)\dot{v}^4\tau^4 \\ &+i\frac{u\mathcal{E}}{120}\left(\frac{1+u}{\gamma^2}\right)\left(3\frac{\dot{B}^2}{B^5}+4\frac{\ddot{B}}{B^4}\right)\dot{v}^5\tau^5 \\ &+i\frac{u\mathcal{E}}{120}\left(1+u+\frac{u^2}{2}\right)\left(9\frac{\dot{B}^2}{B^6}+2\frac{\ddot{B}}{B^4}\right)\dot{v}^7\tau^7 \quad . \end{aligned} \tag{3.29}$$

In the above expression the vector products $\dot{\vec{v}}\cdot\ddot{\vec{v}}$ and $\ddot{\vec{v}}\cdot\dddot{\vec{v}}$ have been replaced by $B\dot{B}$ and $B\ddot{B}$. This is because the only components that $\ddot{\vec{v}}$ and $\dddot{\vec{v}}$ contribute are proportional to $\vec{v}\times\dot{\vec{B}}$ and $\vec{v}\times\ddot{\vec{B}}$, respectively.

Following the mathematical techniques used by Baier and Katkov [27], we introduce angles θ and φ, where θ is the angle between the unit vector $\vec{n}$ of photon propagation and the plane $(\vec{v}, \dot{\vec{v}})$, and φ the angle between the projection of $\vec{n}$ on $(\vec{v}, \dot{\vec{v}})$ and $\vec{v}$, i.e.,

$$\vec{n}\cdot\vec{v} = v\cos\varphi\cos\theta \quad , \quad \vec{n}\cdot\dot{\vec{v}} = \dot{v}\sin\varphi\cos\theta \quad . \tag{3.30}$$

Taking into account the fact that up to terms of highest order in $1/\gamma^2$ the principal contribution comes from small θ and φ, and by shifting the origin of τ to $\tau+\varphi/\dot{v}$, the phase can be written as

$$\begin{aligned} \Phi_0 &= u\mathcal{E}\left[(1-\vec{n}\cdot\vec{v})\tau - \frac{1}{2}\vec{n}\cdot\dot{\vec{v}}\tau^2 + \frac{1}{6}\dot{\vec{v}}^2\tau^3\right] \\ &= \frac{u\mathcal{E}\mu^{3/2}}{2\dot{v}}\left(x+\frac{1}{3}x^3+y+\frac{1}{3}y^3\right) \quad , \end{aligned} \tag{3.31}$$

where

$$\mu \equiv 1 - v^2\cos^2\theta \simeq \frac{1}{\gamma^2}+\theta^2 \quad ,$$

and

$$x = \frac{1}{\sqrt{\mu}}\varphi \quad \text{and} \quad y = \frac{1}{\sqrt{\mu}}\dot{v}\tau \quad .$$

With the definition of Υ in eq. (3.16) the coefficients in the phase can be symbolised by

$$b = \frac{3}{2}\eta = \frac{\alpha}{2\Upsilon}\left(\gamma^2\mu\right)^{3/2} \quad .$$

The radiation intensity associated with head-tail symmetric inhomogeneous field is then

$$\frac{dI_2}{dt} = \frac{4\alpha}{(2\pi)^3}\int k^2 dk d\sin\theta \frac{\mu}{\bar{v}} \int_0^\infty dx \int_0^\infty dy\, G_2 \exp\left\{-ib\left(x + \frac{1}{3}x^3 + y + \frac{1}{3}y^3\right)\right\} \quad . \tag{3.32}$$

Recall that $u = \omega/\mathcal{E}' = \omega/(\mathcal{E}-\omega)$, and $k^2dk = \omega^2 d\omega$, we find that

$$k^2 dk = \frac{\mathcal{E}^3 u^2 du}{(1+u)^4} \quad . \tag{3.33}$$

The intergrations over x and y give Bessel functions of fractional order $K_{1/3}(\eta)$ and $K_{2/3}(\eta)$. For the evaluation of the integral over u it is convenient to introduce the representation [32]

$$\frac{1}{(1+u)^m} = \frac{1}{2\pi i}\int_{\lambda-i\infty}^{\lambda+i\infty} \frac{\Gamma(-s)\Gamma(m+s)}{\Gamma(m)} u^s ds \quad , \tag{3.34}$$

where $1-m < \lambda < 0$. After this transformation the integration over u turns the Bessel functions into gamma functions, multiplied by a factor $(\gamma^2\mu)^{-2(s+n)/3}$ among other things. We can then carry out integration over $\sin\theta \approx \theta$ by the following formula:

$$\int_{-\infty}^{\infty} (\gamma^2\mu)^{-2(s+n)/3}\gamma d\theta = \int_{-\infty}^{\infty} (1+\gamma^2\theta^2)^{-2(s+n)/3}\gamma d\theta = \sqrt{\pi}\frac{\Gamma(3s/2+(3n-1)/2)}{\Gamma(3s/2+3n/2)} \quad . \tag{3.35}$$

All integrations in eq. (3.32) are straightforward, though tedious. The result before carrying out the final integration over s is

$$\frac{dI_2}{dt} = \frac{\alpha\gamma^2}{\pi^{3/2}} \frac{1}{2\pi i} \int_{\lambda-i\infty}^{\lambda+i\infty} ds\, 2^s (3\Upsilon)^s \frac{\Gamma(3s/2+1)}{\Gamma(3s/2+3/2)} \left[\frac{\Gamma(s+4)}{\Gamma(4)} + \frac{\Gamma(s+2)}{\Gamma(2)}\right] \frac{\Gamma(-s)}{\Gamma(s+3)}$$

$$\times \left\{ -\left(\frac{9}{2}\frac{\dot{B}^2}{B^2} + 6\frac{\ddot{B}}{B}\right) \left[\Gamma\left(\frac{s}{2}+\frac{11}{6}\right)\Gamma\left(\frac{s}{2}+\frac{9}{6}\right)\Gamma\left(\frac{s}{2}+\frac{9}{6}\right)\Gamma\left(\frac{s}{2}+\frac{7}{6}\right) \right.\right.$$

$$- \frac{1}{2}\frac{\Gamma(s+3)}{\Gamma(s+2)}\Gamma\left(\frac{s}{2}+\frac{9}{6}\right)\Gamma\left(\frac{s}{2}+\frac{7}{6}\right)\Gamma\left(\frac{s}{2}+\frac{5}{6}\right)\Gamma\left(\frac{s}{2}+\frac{3}{6}\right)$$

$$\left. + \Gamma\left(\frac{s}{2}+\frac{13}{6}\right)\Gamma\left(\frac{s}{2}+\frac{9}{6}\right)\Gamma\left(\frac{s}{2}+\frac{9}{6}\right)\Gamma\left(\frac{s}{2}+\frac{5}{6}\right) \right] \qquad (3.36)$$

$$+ \left(\frac{81}{40}\frac{\dot{B}^2}{B^2} + \frac{9}{20}\frac{\ddot{B}}{B}\right) \left[\frac{256}{3}\Gamma\left(\frac{s}{2}+\frac{11}{6}\right)\Gamma\left(\frac{s}{2}+\frac{9}{6}\right)\Gamma\left(\frac{s}{2}+\frac{9}{6}\right)\Gamma\left(\frac{s}{2}+\frac{7}{6}\right) \right.$$

$$+ \frac{224}{3}\Gamma\left(\frac{s}{2}+\frac{13}{6}\right)\Gamma\left(\frac{s}{2}+\frac{9}{6}\right)\Gamma\left(\frac{s}{2}+\frac{9}{6}\right)\Gamma\left(\frac{s}{2}+\frac{5}{6}\right)$$

$$- \frac{128}{s+3}\Gamma\left(\frac{s}{2}+\frac{15}{6}\right)\Gamma\left(\frac{s}{2}+\frac{13}{6}\right)\Gamma\left(\frac{s}{2}+\frac{11}{6}\right)\Gamma\left(\frac{s}{2}+\frac{9}{6}\right)$$

$$\left. - \frac{216}{9}(s+2)\Gamma\left(\frac{s}{2}+\frac{9}{6}\right)\Gamma\left(\frac{s}{2}+\frac{7}{6}\right)\Gamma\left(\frac{s}{2}+\frac{5}{6}\right)\Gamma\left(\frac{s}{2}+\frac{3}{6}\right) \right] \right\} .$$

where $-1 < \lambda < 0$. The above expression includes only contributions from the $\dot{v}^4 r^4$ and $\dot{v}^7 r^7$ terms in eq. (3.29) because it can be shown that the contribution from the $\dot{v}^5 r^5$ term is significantly smaller, and thus negligible.

The integral over s can be evaluated by closing the contour of integration either to the right for $\Upsilon \ll 1$, or to the left for $\Upsilon \gg 1$. For $\Upsilon \ll 1$, we have

$$\frac{dI_2}{dt} = 0 \quad , \quad \Upsilon \ll 1 \quad , \qquad (3.37)$$

identically. For $\Upsilon \gg 1$ we have, to the leading order in Υ,

$$\frac{dI_2}{dt} = -\frac{\alpha\gamma^2}{\sqrt{\pi}}\Gamma\left(\frac{2}{3}\right)\Gamma\left(\frac{1}{6}\right)\frac{41}{54}\left(\frac{61}{60}\frac{\dot{B}^2}{B^2} - \frac{13}{90}\frac{\ddot{B}}{B}\right)(6\Upsilon)^{-2/3} \quad , \quad \Upsilon \gg 1 \quad . \qquad (3.38)$$

This result is valid for any head-tail symmetric inhomogeneous magnetic field which satisfies the assumptions given previously.

Now we apply eq. (3.38) to the field from a relativistic gaussian bunch with standard deviation σ_z:

$$B(t) = B_0 e^{-2t^2/\sigma_z^2} \quad , \qquad (3.39)$$

where the time of flight of the test electron traversing the oncoming bunch is $t = z/2$. Then we get

$$\frac{dI_2}{dt} = -\frac{32\,\Gamma(2/3)}{243}\alpha m^2(3\Upsilon)^{2/3}\left\{\frac{\Gamma\,(1/6)}{360\sqrt{\pi}}F^2\left[12997\left(\frac{2t}{\sigma_z}\right)^3 - 1804\right]\right\} \quad , \quad \Upsilon \gg 1 \quad , \quad (3.40)$$

where $F \equiv \ell_R/\sigma_z$ is the formation length parameter associated with $\ell_R(\omega)$ in the quantum limit for photon frequency $\omega = \mathcal{E}$:

$$\ell_R(\omega = \mathcal{E}) = \frac{\lambda_c\gamma}{\Upsilon}\left(\frac{\omega_c}{\mathcal{E}}\right)^{1/3} = \left(\frac{3}{2}\right)^{1/3}\frac{\lambda_c\gamma}{\Upsilon^{2/3}} \quad . \quad (3.41)$$

Combining eqs. (3.37) and (3.40) with eq. (3.17), we obtain

$$\frac{dI}{dt} = \frac{dI_0}{dt} + \frac{dI_2}{dt} = \begin{cases} \frac{2}{3}\alpha m^2\Upsilon^2\left(1 + \frac{55\sqrt{3}}{16}\Upsilon + 48\Upsilon^2 + \ldots\right) \quad , & \Upsilon \ll 1 \quad , \\ \frac{32\,\Gamma(2/3)}{243}\alpha m^2(3\Upsilon)^{2/3}\left\{1 - \frac{\Gamma(1/6)}{360\sqrt{\pi}}F^2\left[12997\left(\frac{2t}{\sigma_z}\right)^3 - 1804\right]\right\} \quad , & \Upsilon \gg 1 \quad . \end{cases}$$

(3.42)

Short Magnets and Radiation Reduction

Our result can be appreciated by the following physical arguments: Consider a long uniform magnet with length $L^* \gg \ell_R$. The differential radiation intensity $P(\omega)$ is given by eq. (3.19) and shown by the solid curve in fig. 12. As is introduced in eq. (3.23), classical limit $\Upsilon \ll 1$ corresponds to the situation $\omega_c \ll \mathcal{E}$, meaning the typical frequency of radiated photons is much less than the kinetic energy of the radiating particles. Thus the entire spectrum of eq. (3.19) is observable. On the contrary, the extreme quantum limit $\Upsilon \gg 1$ corresponds to $\mathcal{E} \ll \omega_c$, therefore the spectrum beyond the electron energy is kinematically forbidden, and the observable spectrum scales roughly as $\omega^{1/3}$ as discussed earlier. This cut-off is shown by the vertical dashed line in the figure.

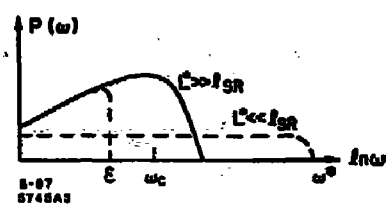

Fig. 12. Radiation spectrum in the two asymptotic limits. For long magnets, $L^* \gg \ell_R$, we have the well-known spectrum in the solid curve. In the opposite limit $L^* \ll \ell_R$, the spectrum approaches a constant. In quantum limit we observe only the low frequency regime.

In the case of nonuniform fields the spectrum differs from that of uniform fields. For the classical limit the problem has been studied by Coïsson [33], and independently by Bagrov, Fedosov and Ternov [34]. It is found that for a short magnet which is comparable in length with ℓ_R, the radiation spectrum is modified in such a way that the low-frequency regime is suppressed in favor of high frequencies beyond ω_c. The total intensity, however, remains the same. The prediction was confirmed by Bossart et al. [35] with observations in SPS at CERN. We can extrapolate this fact by suggesting that when the magnet length $L^* \ll \ell_R$, the spectrum would be a constant independent of ω up to a maximum frequency $\omega^* \sim \omega_c(\ell_R/L^*)$ (see the horizontal dashed curve in fig. 12). Our result for the classical limit shows that the total intensity dI/dt is the same for uniform and gaussian fields. This is a confirmation of the previous studies.

The situation for short magnets is different in the quantum limit. Again, spectrum beyond $\mathcal{E}$ is energetically forbidden. But now that the low frequency regime is suppressed, the overall intensity is reduced. This explains why our dI_2/dt is opposite in sign from dI_0/dt. From eq. (3.42) it can be seen that when $\ell_R \ll \sigma_z$, or when the bunch is very long, $dI_2/dt \to 0$, and we have vanishing correction to the Sokolov–Ternov formula. A pronounced effect occurs when ℓ_R is not much smaller than σ_z.

3.4 Reduction of Quantum Beamstrahlung

First Beamstrahlung Reduction Factor

With the radiation intensities derived in previous sections, we are now ready to estimate the average energy loss during beam-beam collision. Individual e^+e^- scatterings are neglected, and the target bunch acts only to provide a macroscopic field. For the sake of arguments, we will in this section assume a hybrid "cylindrical gaussian" bunch, i.e.,

$$\begin{cases} n_z = \dfrac{1}{\sqrt{2\pi}\sigma_z} e^{-z^2/2\sigma_z^2} \quad , & -\infty < z < \infty \\ n_r = \dfrac{1}{2\sigma_r^2} \quad , & 0 \le r \le 2\sigma_r \quad . \end{cases} \tag{3.43}$$

It is straightforward to show that the local field strength in this case is

$$|\vec{E}|_{R=1} = \frac{eN}{2\sqrt{2\pi}\sigma_r^2\sigma_z} r\, e^{-z^2/2\sigma_z^2} \quad , 0 \le r \le 2\sigma_r \quad . \tag{3.44}$$

The above expression is identical to eq. (3.6) when the approximation of $r \ll \sigma_r$ is taken. We now introduce normalized coordinates as in sec. 2.3,

$$\rho = \frac{r}{\sigma_r} \quad , \quad \zeta = \frac{z}{\sigma_z} \quad , \tag{3.45}$$

then we can define a local beamstrahlung parameter

$$\Upsilon(\rho, z) = \Upsilon_0 \rho e^{-r^2/2} \quad , \tag{3.46}$$

where

$$\Upsilon_0 = \frac{r_e \lambda_c \Gamma N}{\sqrt{2\pi}\sigma_r \sigma_z}$$

is the reference beamstrahlung parameter corresponding to twice the field strength at $(\rho, \zeta) = (1, 0)$ in the target bunch.

Let us first calculate the average energy loss in a semi-uniform field approximation, i.e., dI_0/dt in eq. (3.17). The validity of this assumption for a gaussian current distribution is that the bunch is very long; hence, the field strength changes mildly, i.e., $\dot{B}\tau/B \ll 1$. Equivalently, if a uniform cylinder bunch is invoked, this implies that the end effects are neglected.

Let

$$\epsilon = \frac{\mathcal{E} - \mathcal{E}'}{\mathcal{E}} \tag{3.47}$$

be the fractional energy loss of an electron having impact parameter ρ. Then the average fractional energy loss of the entire bunch is

$$\langle \epsilon \rangle = \frac{\int \int (dI_0/dt) \rho d\rho dt}{\int \rho d\rho} \quad . \tag{3.48}$$

Replacing dt by $(\sigma_z/2)/d\zeta$, since both bunches move toward each other with the speed of light $(c = 1)$, and define

$$\Gamma_0 \equiv \frac{\lambda_c \gamma}{\sigma_z} \quad , \tag{3.49}$$

we find for the classical limit

$$\langle \epsilon_0 \rangle = \frac{2}{3} \frac{\alpha}{\Gamma_0} \Upsilon_0^2 \left[\frac{1}{2} \langle \rho \rangle_c^2 \cdot \int_{-\infty}^{\infty} e^{-\zeta^2} d\zeta \right] \quad , \Upsilon_0 \ll 1 \quad , \tag{3.50}$$

where the classical mean radius is

$$\langle \rho \rangle_c \equiv \left[\frac{\int_0^2 \rho^2 d\rho}{\int_0^2 \rho d\rho} \right]^{1/2} = \sqrt{2} \quad .$$

On the other hand, for the quantum limit

$$\langle \epsilon_0 \rangle = \frac{32 \cdot \Gamma(2/3)}{243} \frac{\alpha}{\Gamma_0} (3\Upsilon_0)^{2/3} \cdot \left[\frac{1}{2} \langle \rho \rangle_q^{2/3} \cdot \int_{-\infty}^{\infty} e^{-\zeta^2/2} d\zeta \right] \quad , \quad \Upsilon_0 \gg 1 \quad , \tag{3.51}$$

where the quantum mean radius is

$$\langle\rho\rangle_q = \left[\frac{\int_0^2 \rho^{5/3} d\rho}{\int_0^2 \rho d\rho}\right]^{3/2} = 2\left(\frac{3}{4}\right)^{3/2} \simeq 1.30 \quad .$$

Notice that the geometric form factors in the two limits are surprisingly close:

$$\frac{1}{2}\langle\rho\rangle_c^2 \cdot \int_{-\infty}^{\infty} e^{-\zeta^2} d\zeta = \sqrt{\pi} \simeq \frac{1}{2}\langle\rho\rangle_q^{2/3} \cdot \int_{-\infty}^{\infty} e^{-\zeta^2/3} d\zeta \simeq 1.03\sqrt{\pi} \quad . \tag{3.52}$$

Assuming from now on the same geometric form factor $\sqrt{\pi}$ in both limits, we then have extremely simple scaling laws for the average fractional energy loss in beamstrahlung:

$$\langle\varepsilon_0\rangle = \begin{cases} \frac{2\sqrt{\pi}}{3}\frac{\alpha}{\Gamma_0}\Upsilon_0^2 \quad , & \Upsilon_0 \ll 1 \quad , \\ \frac{32\sqrt{\pi}\,\Gamma(2/3)}{243}\frac{\alpha}{\Gamma_0}(3\Upsilon_0)^{2/3} \quad , & \Upsilon_0 \gg 1 \quad . \end{cases} \tag{3.53}$$

If one would naively calculate $\langle\varepsilon\rangle$ with a given Υ by using the classical formula for the quantum regime, he would obtain meaninglessly large results before using the correct quantum formula. A beamstrahlung "reduction" factor $H_{\Upsilon 1}$ is thus introduced to account for the change, which is the ratio of the bottom expression to the top expression in eq. (3.53):

$$\lim_{\Upsilon_0 \to \infty} H_{\Upsilon 1}(\Upsilon_0) = \frac{16\Gamma(2/3)}{81}\Upsilon_0^{-4/3} \simeq 0.556\Upsilon_0^{-4/3} \quad ,$$

while $\tag{3.54}$

$$\lim_{\Upsilon_0 \to 0} H_{\Upsilon 1}(\Upsilon_0) = 1 \quad .$$

It is remarkable that this beamstrahlung reduction factor is exactly what one would get by taking the ratio of synchrotron radiation "intensities" in eq. (3.17) for mildly inhomogeneous fields, with Υ_0 as an effective beamstrahlung parameter representing the entire bunch. This is the case only because the geometric form factor does not vary too much in the two limits. It can be shown that this is true even for the transition regime $0.1 \lesssim \Upsilon_0 \lesssim 100$, where we lack a simple analytic scaling law. A numerical plot for the entire range of Υ given by Wilson [2] is shown in fig. 13.

In the literature [21, 2] there is an effective beamstrahlung parameter $\overline{\Upsilon}$ defined based on computer simulation with gaussian bunches,

$$\overline{\Upsilon} = \frac{5}{12}\frac{r_e \lambda_c \gamma N}{\sigma_x \sigma_y}\left(\frac{2\sqrt{R}}{1+R}\right) \quad , \tag{3.55}$$

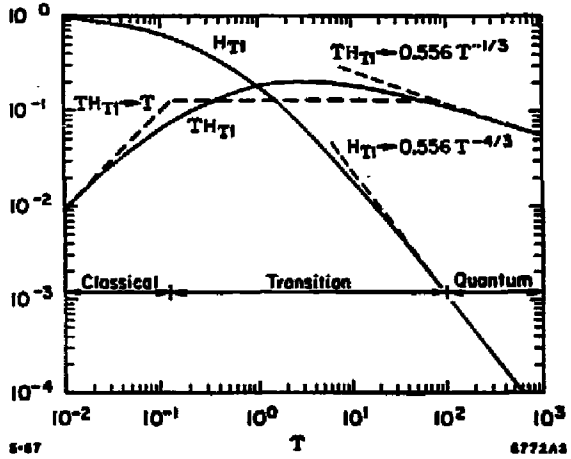

Fig. 13. The beamstrahlung reduction factor H_{T1} and the product TH_{T1} as a function of the scaling parameter T, plotted by P. B. Wilson.

where in the round beam case ($R = 1$), it comes very close to our Υ_0 for a cylindrical gaussian bunch,

$$\frac{\overline{\Upsilon}}{\Upsilon_0} = \frac{5/12}{1/\sqrt{2\pi}} \simeq 1.04 \quad . \tag{3.56}$$

Our analysis in this subsection therefore serves as a theoretical explanation for the previously known facts. Notice, however, that our expressions in eq. (3.53) have conceptually simplified the description: No effective radiation time [2] is necessary, and Γ_0 is defined in a straightforward way without extra numerical factors [21].

Second Beamstrahlung Reduction Factor

As discussed in the earlier sections, the Sokolov–Ternov formula does not include the effect due to the fast variation of the field strength along the particle's trajectory. The correction term derived in sec. 3.3 [cf., eq. (3.42)] indicates that there is an additional beamstrahlung reduction.

To include the correction term we should realize that our perturbation breaks down before dI_0/dt and dI_2/dt becomes equal in magnitude at some point $\zeta = \zeta_c$ from the centroid of the bunch, beyond which the total intensity would turn negative and be certianly unphysical. Since we lack the knowledge on the behavior of higher order terms, we can only estimate the upper bound of the reduction effect by extending dI_2/dt all the way to ζ_c and assuming total suppression beyond that point, as shown schematically in fig. 14. From eq. (3.42) this threshold occurs at

$$\frac{\Gamma(1/6)}{360\sqrt{\pi}} F_0^2 \rho^{-4/3} e^{2\zeta_c^2/3} \left(12997\zeta_c^3 - 1804\right) = 1 \quad , \tag{3.57}$$

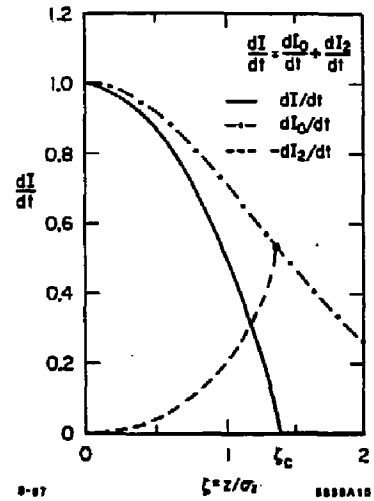

Fig. 14. Radiation intensities as function of longitudinal target bunch coordinate ζ. The dash-dot curve is the Sokolov–Ternov radiation. The dash curve is the negative of our gaussian slope correction. The net intensity is represented by the solid curve. Beyond the point ζ_c where dI_0/dt and $-dI_2/dt$ meet, we assume a total suppression.

where

$$F_0 \equiv \frac{\ell_{R0}}{\sigma_z} = \left(\frac{3}{2}\right)^{1/3} \frac{\lambda_c \gamma}{\Upsilon_0^{2/3} \sigma_z} \tag{3.58}$$

is the reference radiation formation length parameter associated with Υ_0, and is related to F by

$$F(\rho,\zeta) = F_0 \rho^{-2/3} e^{\zeta^2/3} \quad . \tag{3.59}$$

From eq. (3.57) it is obvious that the cut-off ζ_c is radial dependent. For the sake of simplicity in our discussion, we make a further approximation by evaluating ζ_c at the mean impact parameter $\langle\rho\rangle_q = 1.30$. Thus the mean radiation loss is suppressed to

$$\langle\epsilon\rangle_{\zeta_c} = \langle\epsilon_0\rangle_{\zeta_c} + \langle\epsilon_2\rangle_{\zeta_c} \quad , \tag{3.60}$$

where

$$\langle\epsilon_0\rangle_{\zeta_c} = \frac{32 \cdot \Gamma(2/3)}{243} \frac{\alpha}{\Gamma_0} (3\Upsilon_0)^{2/3} \left[\frac{1}{2}\langle\rho\rangle_q^{2/3} \cdot \int_{-\zeta_c}^{\zeta_c} e^{-\zeta^2/3} d\zeta\right] \quad ,$$

and

$$\langle\epsilon_2\rangle_{\zeta_c} = -\frac{32\Gamma(2/3)}{243} \frac{\alpha}{\Gamma_0} (3\Upsilon_0)^{2/3} \left[\frac{1}{2} \frac{\Gamma(1/6)}{360\sqrt{\pi}} F_0^2 \langle\rho\rangle_q^{-2/3} \int_{-\zeta_c}^{\zeta_c} e^{\zeta^2/3} (12997\zeta^2 - 1804) d\zeta\right] \quad .$$

Let us define the second beamstrahlung reduction factor $H_{\Upsilon 2}$ as the ratio of eq. (3.60) to the quantum formula in eq. (3.51):

$$\lim_{\Upsilon_0 \to \infty} H_{\Upsilon 2}(\Upsilon_0, F_0) = Erf\left(\frac{\zeta_c}{\sqrt{3}}\right) - \frac{\sqrt{3}\Gamma(1/6)}{1440\pi} F_0^2 \int_{-\zeta_c}^{\zeta_c} e^{\zeta^3/3}(12997\zeta^2 - 1804)d\zeta \quad , \tag{3.61}$$

where Erf is the error function and

$$\lim_{\Upsilon_0 \to 0} H_{\Upsilon 2}(\Upsilon_0, F_0) = \lim_{F_0 \to 0} H_{\Upsilon 2}(\Upsilon_0, F_0) = 1 \quad . \tag{3.62}$$

With this lengthy expression, it is hard to appreciate the importance of the reduction. As a numerical example, let us take the beam parameters discussed by Himel and Siegrest [16], namely, the Lorentz factor for 5 TeV beams $\gamma = 1 \times 10^7$, number of particles per bunch $N = 1.2 \times 10^8$, bunch size $\sigma_z = 0.4\mu$m and $\sigma_r = 2.5$ Å. With these parameters we find

$$\Upsilon_0 = \frac{r_e \lambda_c \gamma N}{\sqrt{2\pi}\sigma_r \sigma_z} = 5094 \gg 1 \quad , \tag{3.63}$$

and the reference formation length parameter

$$F_0 = \left(\frac{3}{2}\right)^{1/3} \frac{\lambda_c \gamma}{\Upsilon_0^{2/3} \sigma_z} = \frac{0.015\ \mu\text{m}}{0.4\ \mu\text{m}} = 0.0375 \quad . \tag{3.64}$$

The cut-off ζ_c at the mean impact parameter $\langle \rho \rangle_q = 1.30$ turns out to be

$$\zeta_c = 1.49 \quad . \tag{3.65}$$

Plugging in numbers we get

$$\langle \epsilon_0 \rangle_{\zeta_c} = 0.78 \langle \epsilon_0 \rangle_\infty = 11.8\% \tag{3.66}$$

and

$$\langle \epsilon_2 \rangle_{\zeta_c} = -0.11 \langle \epsilon_0 \rangle_\infty = -1.6\% \quad . \tag{3.67}$$

Thus the corrected quantum beamstrahlung average fractional energy loss is

$$\langle \epsilon \rangle \gtrsim \langle \epsilon \rangle_{\zeta_c} = 10.2\% \quad . \tag{3.68}$$

This is substantially different from the previous results. The second reduction factor in this case is

$$H_{\Upsilon 2} = \frac{\langle \epsilon \rangle}{\langle \epsilon_0 \rangle} \simeq 0.67 \quad , \tag{3.69}$$

or reduced from the semi-uniform field approximation by a factor of $\sim 2/3$.

Although our discussion on H_{T2} has been limited to the extreme quantum limit, it is reasonable to assume that this reduction effect occurs to the transition regime as well. Based on the arguments given in sec. 3.3.2, the effect of a short bunch is to suppress the spectrum below ω_c and stretch it to frequencies beyond ω_c. By definition $\Upsilon = 2\omega_c/3\mathcal{E}$, so for Υ as small as $\simeq 1$ the kinetic energy already lies below ω_c and we should expect to see the second reduction.

To conclude, we showed that the average fractional energy loss can be related to the classical synchrotron radiation formula with the reference beamstrahlung parameter Υ_0 as an effective parameter and

$$\langle \epsilon \rangle = \frac{2\sqrt{\pi}}{3}\frac{\alpha}{\Gamma_0}\Upsilon_0^2 \cdot H_{T1} \cdot H_{T2} \quad . \tag{3.70}$$

APPENDIX
QUANTUM FLUCTUATIONS IN BEAMSTRAHLUNG

In this Appendix we list various beamstrahlung quantities of interest to high energy physics and accelerator design. The fluctuation in these quantities arises from the fact that typical number of radiated photons per electron during beam-beam interaction is small in the quantum regime, and not very large (of order several) even in the classical regime like the case of SLC.

Analytic formulas have been derived by Yokoya [22] on the average number of photons radiated per electron $\langle N_\gamma \rangle$, the average fractional energy loss $\langle \epsilon \rangle$ defined in eq. (3.48), the standard deviation of ϵ:

$$\sigma_\epsilon = \langle \epsilon^2 \rangle - \langle \epsilon \rangle^2 \quad . \tag{A.1}$$

the average fractional reduction of the center-of-mass energy $W = S^{1/2} = 2(\mathcal{E}_1 \mathcal{E}_2)^{1/2}$ of two particles in beam 1 and beam 2 at some space-time point:

$$\langle w \rangle = \left\langle \frac{W_0 - W}{W_0} \right\rangle \quad , \tag{A.2}$$

and the standard deviation of w:

$$\sigma_w = \langle w^2 \rangle - \langle w \rangle^2 \quad . \tag{A.3}$$

Following the same spirit, Noble [21] has investigated, in addition to the above quantities, also the average fractional center-of-mass energy squared reduction:

$$\langle s \rangle = \left\langle \frac{S_0 - S}{S} \right\rangle \tag{A.4}$$

and its standard deviation:

$$\sigma_s = \langle s^2 \rangle - \langle s \rangle^2 \quad , \tag{A.5}$$

in computer simulations. Furthermore the average photon energy is introduced as

$$\langle \Omega \rangle = \left\langle \frac{\omega}{\mathcal{E}} \right\rangle \quad . \tag{A.6}$$

Table 1 lists the formulas obtained by the two authors, where

$$A = \frac{\alpha r_e N}{\sigma_\gamma} \, , \quad B = \frac{r_e^3 N^2 \gamma}{\sigma_\gamma^2 \sigma_z} \, , \quad C = \frac{r_e^5 N^6 \gamma^3}{\alpha \sigma_\gamma^2 \sigma_z} = \frac{B^2}{A} \, , \tag{A.7}$$

and

$$Q = \frac{\alpha^4 r_e N^2 \sigma_z}{\gamma \sigma_\gamma^2} \quad . \tag{A.8}$$

The functions $h(\overline{\Upsilon})$ and $g(\overline{\Upsilon})$ are listed in Table 2 for various values of $\overline{\Upsilon}$, and the coefficients a_1, a_2, b, d_1, d_2, d_3 for $\langle \epsilon \rangle \lesssim 0.1$ are listed in Table 3. In all cases no disruption is assumed.

Table 1

Formulas for quantum fluctuation on various physical quantities derived by Yokoya analytically, and deduced by Noble through computer simulation.

	Yokoya		Noble
	$\Upsilon \ll 1$	$\Upsilon \gg 1$	All Υ
$\langle N_\gamma \rangle$	$1.0597A$	$1.554Q^{1/3}$	$\frac{5}{2\sqrt{3}} \frac{\alpha}{\Gamma} h(\overline{\Upsilon})$
$\langle \Omega \rangle$			$\frac{4}{5\sqrt{3}} \frac{g(\overline{\Upsilon})}{h(\overline{\Upsilon})}$
$\langle \epsilon \rangle$	$0.2164B$	$0.395Q^{1/3}$	$\frac{2}{3} \frac{\alpha}{\Gamma} g(\overline{\Upsilon})$
σ_ϵ	$0.4048\langle \epsilon \rangle \left(1 + \frac{31.30}{\langle N_\gamma \rangle}\right)^{1/2}$	$0.193\langle \epsilon \rangle \left(1 + \frac{64.80}{\langle N_\gamma \rangle}\right)^{1/2}$	$a_1\langle \epsilon \rangle \left(1 + \frac{a_2}{\langle N_\gamma \rangle}\right)^{1/2}$
$\langle w \rangle$	$0.4094\langle \epsilon \rangle$	$0.458\langle \epsilon \rangle$	$b\langle \epsilon \rangle (1 + \langle \Omega \rangle)$
σ_w	$0.3146\langle \epsilon \rangle \left(1 + \frac{10.04}{\langle N_\gamma \rangle}\right)^{1/2}$	$0.205\langle \epsilon \rangle \left(1 + \frac{13.20}{\langle N_\gamma \rangle}\right)^{1/2}$	$d_1\langle \epsilon \rangle \left(1 + \frac{d_2}{\langle N_\gamma \rangle}\right)^{1/2}$
$\langle s \rangle$			$2b\langle \epsilon \rangle$
σ_s			$2d_1\langle \epsilon \rangle \left(1 + \frac{d_3}{\langle N_\gamma \rangle}\right)^{1/2}$

Table 2

Representative values of the function $g(\overline{\Upsilon})$ and $h(\overline{\Upsilon})$ in the range $10^{-3} \leq \overline{\Upsilon} \leq 10^3$.

$\overline{\Upsilon}$	$g(\overline{\Upsilon})$	$h(\overline{\Upsilon})$
10^{-3}	9.94×10^{-7}	9.99×10^{-4}
10^{-2}	9.45×10^{-5}	9.91×10^{-3}
10^{-1}	6.55×10^{-3}	9.30×10^{-2}
1	1.82×10^{-1}	7.16×10^{-1}
10	1.84	4.24
10^2	1.11×10^1	2.13×10^1
10^3	5.56×10^1	1.01×10^2

Table 3

Behavior of the energy loss coefficients a_i, b and d_i as a function of the beam radiation parameter $\overline{\Upsilon}$ when $\langle \epsilon \rangle \lesssim 0.1$.

$\overline{\Upsilon}$	a_1	a_2	b	d_1	d_2	d_3
$\lesssim 10^{-2}$	0.41	30	0.42	0.32	10	10
10^{-1}	0.38	30	0.43	0.31	10	10
1	0.31	33	0.44	0.27	14	10
10	0.25	43	0.45	0.24	18	11
10^2	0.22	53	0.46	0.22	22	12
$\gtrsim 10^3$	0.20	63	0.47	0.21	26	13

$\overline{\Upsilon}$ is defined in eq. (3.55) as

$$\overline{\Upsilon} = \frac{5}{12}\,\frac{r_e \lambda_c \gamma N}{\sigma_x \sigma_y}\left(\frac{2\sqrt{R}}{1+R}\right) \simeq \Upsilon_0 \quad . \tag{A.9}$$

The symbol Γ is related to our Γ_0 [eq. (3.49)] by

$$\Gamma = \frac{9}{16}\,\frac{\lambda_c \gamma}{\sigma_x} \simeq \frac{1}{\sqrt{\pi}}\,\Gamma_0 \quad , \tag{A.10}$$

i.e., the geometric form factor $\sqrt{\pi}$ has been absorbed into Γ.

More recently, Amaldi [36] introduces simple scaling laws that reasonably reproduce the formulas in Table 1:

$$\langle \epsilon \rangle \simeq \left(\frac{4}{5}\right)^2 2\,\frac{\alpha}{\Gamma_0}\,\overline{\Upsilon}^2 \left(1 + \overline{\Upsilon}^{1/2} + \frac{3}{2}\,\overline{\Upsilon}\right)^{-4/3} \quad , \tag{A.11}$$

$$\langle N_\gamma \rangle \simeq 2\langle \epsilon \rangle \left(1 + \overline{\Upsilon}^{1/2} + \sqrt{\pi}\,\overline{\Upsilon}\right) \Big/ \overline{\Upsilon} \quad , \tag{A.12}$$

$$\langle \Omega \rangle \simeq \frac{1}{2}\,\overline{\Upsilon}\left(1 + \overline{\Upsilon}^{1/2} + \sqrt{\pi}\,\overline{\Upsilon}\right) \quad , \tag{A.13}$$

and

$$\sigma_w \simeq \frac{1}{9}\,\langle \epsilon \rangle \left(2 + e^{-\overline{\Upsilon}/3}\right)\left[1 + \frac{10 + \sqrt{3}\,\ln(10\overline{\Upsilon} + 1)}{\langle N_\gamma \rangle}\right]^{1/2} \quad . \tag{A.14}$$

REFERENCES

1. *SLC Design Handbook*, SLAC, Stanford, CA (Dec. 1984); SLAC–Report–229 (June 1980).
2. P. B. Wilson, SLAC–PUB–4310 (May 1987).
3. U. Amaldi, Nucl. Ins. Meth. **A243**, 312 (1986).
4. Y. H. Chin, DESY Report (1987).
5. This idea was recently suggested by R. Palmer.
6. K. Yokoya, private communications.
7. R. Hollebeek, Nucl. Ins. Meth. 184 (1981).
8. R. Hollebeek and A. Minten, SLAC Internal Report, CN–301 (June 1985).
9. A. Minten, SLAC Internal Report, CN–305 (June 1985).
10. K. Yokoya, SLAC Internal Report, AAS–27 (March 1987).
11. R. Palmer, SLAC Internal Report, AAS–30 (1987).
12. P. Chen and K. Yokoya, SLAC–PUB–4339 (1987).
13. W. M. Fawley and E. P. Lee, Lawrence Livermore National Laboratory Report (1987).
14. K. Yokoya, KEK Report 85–9 (1985).
15. R. Richter, IEEE Trans. Nucl. Sci. NS–32, 3828 (1985).
16. T. Himel and J. Siegrest, *Laser Acceleration of Particles*, eds. C. Joshi and T. Katsouleas, AIP Conf. Proc. No. 130 (1985).
17. W. Schnell, CERN–LEP–RF/86–06 and CLIC Note 13, 1986. The parameters stated in our paper is a recent modification by Schnell.
18. P. Chen, in *Physics at Future Accelerators*, ed. J. Mulvey, CERN 87–07, Vol. I (1987).
19. R. Blankenbecler and S. D. Drell, Phys. Rev. D 36, 277 (1987).
20. M. Jacob and T. T. Wu, CERN–TH/87–61 (1987).
21. R. J. Noble, SLAC–PUB–3871 (1986), to appear in Nucl. Inst. Meth.
22. K. Yokoya, Nucl. Inst. Meth. **A251**, 1 (1986).
23. P. Chen, SLAC–PUB–4391 (1987), to appear in the Proceedings of the Workshop on *New Developments in Particle Acceleration Techniques*, Orsay, France (June 1987).
24. F. Klein, Zeitschrift der Physik 53, 157 (1929).
25. P. Chen and R. J. Noble, SLAC–PUB–4050 (1986).
26. M. Bassetti, J. Bosser, R. Coïsson, M. Gygi–Hanney, A. Hofmann and E. Keil, IEEE Trans. Nucl. Sci. NS–30, 2182 (1983).
27. V. N. Baier and V. M. Katkov, Soviet Phys. JETP 26, 854 (1968); and Soviet Phys. JETP 28, 807 (1969).
28. J. Schwinger, Proc. National Academy of Sci. 40, 132 (1954).
29. A. A. Sokolov, N. P. Klepikov and I. M. Ternov, Soviet Phys. Doklady, 89, 665 (1953).
30. A. A. Sokolov and I. M. Ternov, *Synchrotron Radiation*, Pergamon Press (1967).
31. W. Panofsky, private communications (1985).
32. V. N. Baier, V. M. Katkov and V. M. Strakhovenko, INP–Novosibirsk 87–26 (1987).
33. R. Coïsson, Optics Comm. 22, 135 (1977) and Phys. Rev. A 20, 524 (1979).
34. V. G. Bagrov, N. I. Fedosov and I. M. Ternov, Phys. Rev. D 28, 2464 (1983).
35. R. Bossart, J. Bosser, L. Burnod, R. Coïsson, E. D'Amico, A. Hofmann and J. Mann, Nucl. Inst. Meth. 164, 374 (1979).
36. U. Amaldi, CERN–EP/87, in these Proceedings.